AD-A220 108

MENTATION PAGE

Form Approved OMB No. 0704-0188

i estimated to average I nour per resonne, including the time for reviewing instructions, searching existing data sources, ig and reviewing the collection of information. Send comments regarding this burden estimate or any other assect or this ig this burden, to Washington Headquarters Services, Directorate for information Operations and Resorts, 1215 Jefferson to the Office of Management and Budget, Paperwork Reduction Project (0704-0188), Washington, OC 20583.

1. AGENCY USE ONLY (Leave blank,

February, 1990

3. REPORT TYPE AND DATES COVERED

Final Report - 89-90

4. TITLE AND SUBTITLE

Fourth International Conference on the Science and Technology of Zirconia (ZrO₂ IV)

5. FUNDING NUMBERS

& AUTHOR(S)

I-Wei Chen

AF0SR-89-0366 レリングヒ

2306

7. PERFORMING ORGANIZATION NAME(S) AND ADDRESS(ES)

University of Michigan Department of Materials Science & Engineering 2086 Dow Building 2300 Hayward Street Ann Arbor, MI 48109-2136

REPORT NUMBER

AFOGR-TR. 90-0350

9. SPONSORING/MONITORING AGENCY NAME(S) AND ADDRESS(ES)

Dr. Liselotte J. Schioler

10. SPONSORING / MONITORING AGENCY REPORT NUMBER

Air Force Office of Scientific Research File Line Bolling Air Force Base TVC. 2033

AFUSR-89-0366

11. SUPPLEMENTARY NOTES

Unlimited |

MAR 28 1990

12b. DISTRIBUTION CODE

13. ABSTRACT (Maximum 200 words)

12a DISTRIBUTION / AVAILABILITY STATEMENT

The Fourth International Conference on the Science and Technology of Zirconia (ZrO2 IV) was held at Anaheim, California in November, 1989. One hundred twenty (120) papers were presented on topics covering fuel cells, phase transformation, processing, sensors, defects, fracture, fatigue, creep, and superplasticity. Trends in zirconia research are summarized. It is suggested that zirconia has begun to attain the status of "classical" ceramics, like Al₂0₃ and UO₂, and will continue to offer current and future scientific research opportunities.

15. NUMBER OF PAGES

14. SUBJECT TERMS

Zirconia; Fuel Cell; Phase Transformation; Sensors; Processing; Toughening; Fracture, Fatigue, Superplasticity, Microstructure

16. PRICE CODE

17. SECURITY CLASSIFICATION OF REPORT

18. SECURITY CLASSIFICATION OF THIS PAGE Unclassified

19. SECURITY CLASSIFICATION OF ABSTRACT Unclassified

20. LIMITATION OF ABSTRACT

NSN 7540-01-280-5500

Unclassified

Standard Form 298 (Rev. 2-89)

Unlimited

FINAL REPORT

The Fourth International Conference on The Science and Technology of Zirconia (ZrO₂IV) was held from November 1 to November 3, 1989, in Anaheim, California. The conference followed the successful meetings on the same topic held in Cleveland, 1980, Stuttgart, 1983, and Tokyo, 1986.

The organizers of the conference were A.H. Heuer, I-Wei Chen, and W. Worrell. The Basic Science Division of the American Ceramic Society and the High Temperature Material Division of the Electrochemical Society were the sponsors. The conference was held as a symposium in the umbrella meeting called The First International Ceramic Science and Technology Congress sponsored by The American Ceramic Society. Supplementary financial support was received from the Air Force Office of Scientific Research and from Army Research Office. Additional funds for student support was received from the ceramic industry.

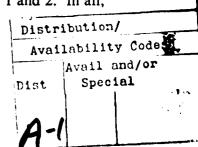
The following sections were held:

- --Solid Oxide Fuel Cells, chaired by W.L.F. Weppner
- --Phase Transformations: Thermodynamics, Metastability and Stress-Induced
 Transformations, chaired by R.C. Garvie
- -- Processing and Microstructural Control, chaired by F.F. Lange
- --Oxygen Sensors and Electrochemical Catalysis, chaired by W.L. Worrell
- --Defects and Their Role in Ionic Conductivity, chaired by A. Dominguez-Rodriguez
- --Mechanical Properties/Microstructural Correlation, chaired by M. Rühle
- -- Creep, Fatigue and Superplasticity, chaired by A.V. Virkar

In addition, two evening poster sessions were held on November 1 and 2. In all,

120 papers were presented.





By comparing the presentations between the present and the last two zirconia conferences, the following observations can be made:

- --Electrolytic applications are once again regarded as commercially attractive, helped by improvement in fabrication methods and material reliability;
- --Phase transformation studies have matured and the remaining issues on phase stability fields appear to be settled. However, a more fundamental physical and chemical understanding of the role of stabilizers is almost totally lacking;
- --Major progress in processing and microstructural studies is related to utilizing the unique features of zirconia for model studies; in particular, understanding of grain growth of nonstoichometric oxides and of coarsening in general has been advanced;
- --R-curve behavior and cyclic fatigue have been well-appreciated since 1986; however, for very high toughness zirconia, a predictive model does not yet exist;
- --Grain boundary effects are receiving renewed interest in view of the progress in low temperature conductivity and superplasticity;
- --Zirconia is capable of both very high creep resistance, in precipitation-hardened single crystals, and very low flow stress, in ultrafine-grained TZP.

We may conclude that while zirconia science is becoming better-established, and zirconia technology is continuing to be developed, zirconia has begun to attain the status of "classical" ceramics like alumina and urania. In this state, it will be studied and referred to as a model system to test various paradigms of current and future interest in ceramic science.

No conference proceeding was published. Copies of the abstracts and a list of authors are attached as Appendix A and B.

FOURTH INTERNATIONAL CONFERENCE ON THE SCIENCE AND TECHNOLOGY OF ZIRCONIA

Sponsored by the Basic Science Div., Cosponsored by the High Temperature Material Div. of the Electrochemical Society Organized by A. H. Heuer, Dept. of Materials Science & Engrg., Case Western Reserve University, Cleveland, OH

California Pavilion C Anaheim Hilton

Wednesday Morning • November 1

"Solid Oxide Fuel Cells"

Session Chair: Werner L. F. Weppner, Max-Planck-Institut fur Festkorperforschung, Stuttgart, FRG

8:00-8:40 a.m.-(1-SIV-89C)

RECENT ADVANCES IN ZIRCONIA-BASED FUEL CELLS, S. C. Singhal, Westinghouse R&D Center, Pittsburgh, PA 15235

The design and operation of the tubular high temperature fuel cell, utilizing a thin film of yttria-stabilized zirconia as the electrolyte, is described. The functional requirements of the various cell components are reviewed, and the materials and fabrication processes selected for each cell component are discussed. Representative performance curves of the cell at different temperatures, fuel utilizations and current densities are presented, and any potential long-term interactions at component interfaces are reviewed. Finally, recent progress in the use of these fuel cells for power generation is described.

This work has been supported both by the U.S. Department of Energy under Contract No. DE-AC21-80ET17089 and the Westinghouse Electric Corporation.

9:20-9:40 a.m.-(3-SIV-89C)

CHEMICAL VAPOR DEPOSITION OF YTTRIA-DOPED ZIRCONIA FILMS FOR SOLID OXIDE FUEL CELL APPLICATIONS, K.A. Klemm and P.A. Lessing, Materials and Metallurgical Engineering Department, New Mexico Institute of Mining and Technology, Socorro, NM, 87801

Thin films of ZrO₂-Y₂O₃ were fabricated using cold-wall chemical vapor deposition. Organometallic beta-diketone chelate compounds of zirconium and yttrium (Zr(tfacac), and Y(thd)3) were used as volatile precursors. Deposition was conducted using atmospheric and reduced (7-12 torr) pressures, at temperatures between 450 and 750°C with and without the use of H₂O and O₂ as oxidants. Conditions were mapped that lead to amorphous coatings, crystalline coatings from heterogeneous surface growth, and crystalline coatings from homogeneous vapor phase nucleation. Deposition rates and coating morphologies were modeled. The heterogeneous deposition reaction is first order, not strongly activated by temperature, and the coatings are consistent with the "structure zone model". The 2r02 deposition rate was suppressed when $\Upsilon(\text{thd})_3$ was added for Y_2O_3 doping.

8:40-9:20 a.m.-(2-SIV-89C)

DEVELOPMENT OF PLANAR ZIRCONIA OXYGEN PUMPS AND FUEL CELLS, Ashok V. Joshi and Ashok C. Khandkar, Ceramatec, Inc., 2425 South, 900 West, Salt Lake City, Utah, 84119

Planar, thin film zirconia electrolytes allow higher performance than tubular technologies. However, planar thin film device technology is quite complex due to various practical difficulties such as manifolding, high temperature seal materials and bipolar interconnectors. Ceramatec has developed low cost, planar, thin film electrolyte fabrication technology which is being used to develop flat plate oxygen pumps and fuel cells. Zirconia "membranes" as thin as 75 microns x 200 cm are used to develop high power density (300-500 mW/cm²) capability. Multi-cell stacks have been built and tested. Materials development, design issues and performance of such devices will be presented. Problems and potential solutions to performance stability and device reliability will be discussed. The importance of integration of different technologies for successful device development will be emphasized.

9:40-10:00 a.m.-(4-SIV-89C)

GROWTH RATES, MECHANISM AND MORPHOLOGY OF ELECTROCHEMICALLY VAPOR DEPOSITED YTTRIA-STABILIZED ZIRCONIA THIN FILMS, M.F. Carolan* and J.N. Michaels, Dept of Chemical.Engineering, Univ of California, Berkeley, CA 94720

Yttria stabilized zirconia (YSZ) thin films were deposited on porous alumina by feeding water vapor and a mixture of yttrium chloride and zirconium chloride vapors to opposite faces of the substrate. Film deposition occurred and the result is best explained by a reaction model that is positive order in metal chloride concentration and zero order in water vapor. These results are consistent with a proposed model where film growth is limited by electron transport through the growing film. At a deposition temperature of 1100°C, the films exhibit smooth surfaces and no preferred crystallographic orientation. At deposition temperatures of 1075°C and below, the films exhibit a highly faceted surface and grow preferentially in the <110> direction.

10:00-10:40 a.m.-(5-SIV-89C)

YTTRIA TETRAGONAL ZIRCONIA POLYCRYSTALLINE ELECTROLYTES FOR SOLID STATE ELECTROCHEMICAL CELLS, S.P.S. Badwal, CSIRO Division of Materials Science and Technology Clayton Victoria 3168 Australia

Yttria containing tetragonal zirconia polycrystalline (Y-TZP) ceramics with and without the addition of alumina have excellent thermomechanical properties. Moreover, the lattice conductivity of Y-TZP materials is comparable or better than that of fully stabilized zirconia. Because of this unique blend of properties, these materials are of enormous interest in high power density (thick film self-supporting structures) fuel cells and partial oxidation reactors in addition to advanced structural applications. However, both the resistivity (especially the grain boundary) and phase stability are affected by the powder preparation and ceramic fabrication techniques. The contribution from grain boundary resistivity in general is large and is influenced by several processing variables. In this paper we discuss the conducting properties of Y-TZP materials and their suitability as electrolytes for solid state electrochemical cells.

10:40-11:20 a.m.-(6-SIV-89C)

MIXED-CONDUCTING YTTRIA-STABILIZED ZIRCONIA-TITANIA ELECTRODES FOR SOLID OXIDE FUEL CELLS, S.S. Liou and W.L. Worrell, Department of Materials Science and Engineering, University of Pennsylvania, Phildelphia, PA 19104

Novel mixed-conducting yttria-stabilized zirconia-titania solutions have been synthesized and electrically characterized. The dissolution of titania into yttriastabilized zirconia increases significantly the percentage of electronic conductivity in this oxygen-ion conductor. The electronic conductivity has been measured at temperatures between 800 and 1000°C using a platinum electrode to block oxygen-ion transport. The percentage of electronic conductivity is calculated from the electronic/total electrical conductivity ratios and from separate Emf cell measurements. The percentage of electronic conductivity increases with increasing titania concentration and with decreasing temperature. The results are used to estimate the electrode current densities of these new mixed-conducting oxides in solid oxide fuel cells.

California Pavilion C Anaheim Hilton

Wednesday Afternoon • November 1

"Phase Transformations: Thermodynamics, Metastability and Stress-Induced Transformations"

Session Chair: Ron C. Garvie, CSIRO, Div. of Materials Science and Technology, Clayton, Victoria, Australia

1:40-2:20 p.m.-(7-SIV-89C)

PHASE STABILITY AND TRANSFORMATION OF THE METASTABLE TETRAGONAL PHASES PREPARED BY RAPID QUENCHING OF MELTS IN THE SYSTEMS ZrO_-RO., *M.YOSHIMURA,M.YASHIMA,T.NOMA and S.SŌMIYA; 5 Res.Lab.Eng.Mat.,Tokyo Ins.Tech.,Yokohama,Japan.

Rare-earth-doped zirconia were melted and rapidly quenched with a hammer-anvil apparatus (cooling rate>105K/s). The formation region of metastable tetragonal ZrO2 is from 2 to 14mol% of RO_{1,5} regardless of the species of dopants. The unit cell volume of the tetragonal phases increased with the increase of ionic radii and contents of R³. The tetragonality (axial ratio c/a) is dependent on the contents of dopants but independent of species of dopants. Under the application of external stress by milling or chemical corrosion, the transformability of the tetragonal phases into monoclinic, strongly corresponds to the c/a.It seems to indicate that a certain amount of accumulated stresses are needed to exceed the potencial barrier to transform from tetragonal into monoclinic symmetries. The Tom temperatures also correspond to the tetragonality strongly, but weakly corre elate with the unit cell volume.

2:20-2:40 p.m.—(8-SIV-89C)

CRYSTAL CHEMISTRY AND PHASE STABILITY OF ZIRCONIA SOLID SOLUTIONS, T.S. Sheu and T.Y. Tien*, Department of Materials Science and Engineering, The University of Michigan, Ann Arbor, Michigan, 48109-2136. (313) 764-9449.

Solid solubility limits, lattice distortion and stability of tetragonal zirconia solid solutions and stability of cubic fluorite zirconia solid solutions were studied. Systems studied in-clude $ZrO_2-M_2O_3$ and ZrO_2-MO , where $M^{3+}=Y$, Yb, In and Sc and M^{2+} =Ca and Mg. Compositions in the tetragonal and cubic plus tetragonal phase field in all of the systems studied formed single phase solid solution with cubic fluorite structure at high temperatures. These cubic solid solutions will decompose to cubic plus tetragonal or change to single phase tetragonal depending on the quenching rate. It was also found that the stability of the tetragonal phase depends on the tetragonality (c/a ratio) of the solid solution.

2:40-3:00 p.m.-(9-SIV-89C)

SMALL ANGLE NEUTRON SCATTERING IN THE BULK INTERIOR OF ZrO₂ DURING THE MONOCLINIC

TETRAGONAL TRANSFORMATIONS, + S.-K. Chan, *
J. E. Epperson, Y. Fang, and Z. Li, Materials Science Division, Argonne National Laboratory, Argonne, IL 60439

Small angle neutron scattering experiment has been carried out on pristine single crystals of monoclinic ZrO₂ under equilibrium condition during step-wise heating from 800°C to 1300°C and again during cooling. This experiment provided for the first time in situ measurements in the bulk interior of the internal surfaces generated by nucleation and growth as a function of temperature for the monoclinic ≠ tetragonal transformations. The results will be discussed in relation to the nature of the transformation, the stability limits of the monoclinic and tetragonal phases and the onset of the forward and the reverse transformations.

*Work supported by U.S. DOE, BES-Materials Science, under Contract W-31-109-ENG-38.

3:20-3:40 p.m.-(11-SIV-89C)

DEFORMATION BEHAVIOR OF DOPED CERIA-STABILIZED ZIRCONIA IN UNIAXIAL COM-PRESSION, K.M.Prettyman* and A.V. Virkar, University of Utah, 304 EMRO, Salt Lake City, UT 84112 801-581-3429; R.A.Cutler, Ceramatec Inc., 2425 S 900 W, Salt Lake City, UT 84119

We have studied TZP materials that transform reversibly or irreversibly, depending on dopant level, when loaded in compression. The deformation is studied by mounting multiple strain gage rosettes on different faces of the sample, monitoring strain in the axial and transverse directions. Change in volume during loading and unloading is calculated. XRD patterns are obtained before and after loading and after post-stress annealing to determine texture formation and phases present. Mechanical properties of the materials are correlated with stressstrain response.

3:00-3:20 p.m.-(10-SIV-89C)

NEUTRON DIFFRACTION STUDIES OF ORTHORHOMBIC ZIRCONIA IN MAGNESIA-PARTIALLY STABILISED ZIRCONIA, R.J. Hill, CSIRO Mineral Products, Port Melbourne 3207, Australia; C.J. Howard and E.H. Kisi, Australian Nuclear Science and Technology Organisation, Lucas Heights 2234, Australia.

In certain high-toughness Mg-PSZ, a tetragonal to orthorhombic transformation occurs on cooling below about 200K. The crystal structure of the orthorhombic phase has been established by analysis of the neutron powder diffraction pattern. Neutron diffraction patterns have been recorded at temperatures ranging from 20K to 670K, allowing the tetragonal to orthorhombic transformation on cooling and the reversion of the orthorhombic to tetragonal on subsequent heating to be followed in detail.

3:40-4:00 p.m.-(12-SIV-89C)

STRESS STATE EFFECT ON TRANSFORMATION-TOUGHENED ZIRCONIA, J.S. Cherng* and I-Wei Chen, University of Michigan, Ann Arbor, MI 48109-2136. (313) 763-6661.

Due to the dilatant nature of the t-to-m transformation, the stress state has a profound effect on the mechanical behavior of transformation-toughened zirconia ceramics. Here we summarize our data, hitherto unpublished, on yield stress, bend strength, reversibility, and fracture toughness under different stress states and compare them with current models of transformation plasticity and transformation toughening.

4:00-4:20 p.m.-(13-SIV-89C)

THE EFFECT OF NORMALITY IN TRANSFORMATION TOUGHENING, John C. Lambropoulos, Department of Mechanical Engineering, University of Rochester, Rochester, NY 14627.

Recently measured (by Chen and coworkers) constitutive relations for transformation toughened zirconia ceramics are used in order to predict the effect on the fracture toughness enhancement of the lack of normality of the plastic strain increments to the yield surface. The incremental constitutive relation and the yield surface fully couple dilatational and shear effects. The issue of normality is discussed within the context of statuonary and steadily growing cracks, and of the localization of transformation in microscopic bands. Normality is also discussed from the point of view of internal variable theory (the internal variable being identified with the volume fraction of transformed material) which elucidates the physical mechanisms, and in particular nucleation of the transformation and autocatalysis, which lead to lack of normality. The effect of normality on the fracture toughness enhancement and on the tearing modulus dK/da is also discussed.

Work supported by National Science Foundation Grants MSM-8857096 and MSM-8503984.

4:40-5 00 p.m.-(15-SIV-89C)

TRANSFORMATION PLASTICITY IN MG-PSZ AND Y-TZP USING A SPLIT HOPKINSON PRESSURE BAR TECHNIQUE, W.P. Rogers* and S. Nemat-Nasser, Department of Applied Mechanics and Engineering Sciences, R-011, University of California San Diego, La Jolla, CA 92093.

Transformation plasticity is studied in polycrystaline Mg-PSZ, single crystal Mg-PSZ, and Y-TZP. The split Hopkinson pressure bar, modified for ceramic materials, provides accurate measurements of axial and transverse strain under uniaxial compressive stress. The macroscopic shear and dilatational components of transformation yielding are related to microscopic deformation mechanisms associated with the stress induced tetragonal to monoclinic phase transformation, such as shear localization and microcracking. These deformation mechanisms are characterized using optical interference, X-ray diffraction, and electron microscopy.

4:20-4:40 p.m.--(14-SIV-89C)

TRANSFORMATION TEXTURES IN ZIRCONIA K. J. Bowman, Purdue University, W. Lafayette, IN 47907 and I-W. Chen, The University of Michigan, Ann Arbor, MI 48109

The large shear component of the t->mtransformation in zirconia causes a stressinduced preferred orientation of the t and mvariants in addition to a twin texture within the transformed monoclinic phase. Although the degree of texture may differ for tensile versus compressive loading, a preferred orientation of m twins is apparent under all known deformation conditions. Such a preferred orientation is an indication of the shear contribution to transformation and thereby the role of shear in transformation toughening. In addition to model and experimental results for transformation textures in zirconia, the implications of transformation textures on the performance of zirconia ceramics will be discussed. This work is supported by the National Science Foundation Grant No. DMR-8807024 and DMR-8819186.

Wednesday Afternoon • November 1 Poster Session — 5:00-6:40 p.m.

"Electrolytic Behavior and Defects"

Session Chair: Roger H. French, E. I. du Pont de Nemours & Co., Central Research, Wilmington, DE 19880

(1-SIVP-89C)

FHE ORIGIN OF CUBIC ZIRCONIA DEFECTS IN Y-TZP CERAMICS, M. P. Thomas*; E. P. Butler*; C. J. Norman+; M. C. Thornton*; *Alcan International Ltd, Banbury Laboratories, Banbury, Oxon OX16 7SP England; +Magnesium Elektron Ltd, Regal House, London Rd, Twickenham TW1 3QA England

Y-TZP powders with nominally the same Y and impurity content can produce ceramics with widely different mechanical properties, due to the presence of clusters of cubic zirconia which act as critical flaws. One possible origin concerns Y concentration variation in the starting powder.

Two ceramic powders, of which one produced a ceramic containing few isolated cubic grains, the other isolated grains and clusters of cubic phase, were examined using STEM and TEM. The results showed differences in composition and particle size between the two powders. In one case a correlation between composition and particle size was found. Whilst the origin of the differences is unclear, we have suggested a possible mechanism for Y distribution during sintering.

(2-SIVP-89C)

ELECTRICAL POROPERTIES OF YTTRIA-STABILLIZED ZIRCONIA, R.Yazdanı-Rad and F.Moztarzadeh. Materials and Energy Research Center, P.O.Box 14155-4777, Tehran. IRAN.

Electrical conduction in the ZrO $_2$ -Y $_2$ O $_3$ system is due_almost entirely to the high mobility of O 2 ions via vacanices. The addition of more than 9 mol % Y $_2$ O $_3$ to zirconia results in the fluorite-type phase, as reported. To determine electrical was made. The results indicate that the minimum resistivity of stabilized zirconia can be obtained by adding minimum quantity of Y $_2$ O $_3$ required for the formation of fluorite-type solid solution.

(3-SIVP-89C)

CALCULATION OF OXYGEN-ION MOBILITY IN $2\text{rO}_2-Y_{2}\text{O}_3$ SOLID SOLUTIONS, F.Moztarzadeh & Zohreh Akhavin Mohamadi, Materials & Energy Research Center, P.O.Box 14155-4777, Tehran, IRAN.

The solid solution of $2r0_2-Y_20_3$ is known as "Stabilized Zirconia" and has many applications, including refractory material for solid electrolyte, fuel cells and more recently used as a precise oxygen sensors in automotive and steel manufacture. In this work, the rate of oxygen-ion mobility has been investigated by mesuring the electric conductivity of different samples of 2rO_2 - $Y_2\text{O}_3$ solid electrolyte. The results show that the mobility decreases with increasing the rate of Y_2O_7 in the media of solid solution of fluorite-type structure. This effect was unusual and is subject to more studies. Detail of this unusual finding will be pointed out later on.

(4-SIVP-89C)

EFFECTS OF MICROSTRUCTURE ON THE PHOTOLUMINESCENCE BEHAVIOR OF STABILIZED ZIRCONIA, P. Camagni, N. Cmenetto, G. Samoggia*, M. Scagliotti, Dipartimento di Fisica "A. Volta" dell'Universita, Pavia, Italy

Samples of the luminescence pattern of different yttria-stabilized zirconia display nearly the same features. This pattern is tentatively attributed to intraionic transitions of the trivalent erbium ion. A preliminary analysis of laser excited time resolved luminescence in erbia stabilized zirconia shows the existence of two different lifetimes associated with two intense erbium bands (19200 and 15200 cm⁻¹ structures), which are characterized by the same excitation spectrum. The observation of an anomalously short lifetime (100 nsec.) for the higher energy band indicates an increase of the oscillator strength with respect to theoretical predictions for the cubic matrix. These studies are being extended to low temperatures to obtain data on the environment of the fluorescent probe and possible modifications.

(5-SIVP-89C)

LATTICE PARAMETERS AND ICN-PACKING MODEL FOR UNIT CELL VOLUME OF METASTABLE TETRAGONAL PHASES IN THE SYSTEM ZrO.-RO. 57 M.YASHIMA, M.YCSHIMURA,N.ISHIZAWA and S.SOMIYA, Research Latoratory of Engineering Materials, Pokyo Institute of Technology, Midori, Yokohama, Japan.

The cube root of unit cell volumes of metastable tetragonal phases, which are formed by rapid quenching of melts in the system ZrO_2-RO_1 , give linear relations with the contents of RO_1 . The slopes of these linear relations have been interpreted by an ion packing model, which is an extension of the Aleksandrov model. The cube root of unit cell volume, interatomic distances and the average coordination number can be calculated using ionic radii after Shannon and the distribution of the coordination number of cations. The caluculated average coordination number of 6.5, Y-O distance of 0.23 nm and Y-cations distance of 0.370 nm, are in good agreement with the the experimental results reported previously by EXAFS after Morikawa et al.

(7-SIVP-89C)

IMPEDANCE SPECTROSCOPICAL CHARACTERIZATION OF CRACKS IN CERAMICS, L. Dessemond* and M. Kleitz, Laboratoire d'Ionique et d'Electrochimie du Solide de Grenoble, E.N.S.E.E.G., Domaine Universitaire, B.P. 75, 38402 Saint Martin D'Heres Cedex, France, (00.33).76.82.65.00.

The Impedance Spectroscopy applied to ceramics is sensitive to microstructure and extended defects. investigated responses to mechanical cracking of various parameters which can be determined from the impedance diagrams. Cracks have been induced by three-point bending tests and Vickers indentation in MgO-Partially Stabilized Zirconia and Yttria-Stabilized Zirconia sintered materials. Measurements were performed in the 300-750°C temperature range and over the frequency range 5 to 1.3x10 Hz. Unexpected electrical conductivity increase has been observed after mechanical cracking. Impedance Spectroscopy can be used as a non-Impedance destructive characterization technique.

(6-SIVP-89C)

PHASE STABILITY AND CONDUCTIVITY STUDIES IN YTTRIA-SCANDIA-ZIRCONIA, F.T. Ciacchi, S.P.S. Badwal* and J. Drennan, CSIRO, Division of Materials Science & Technology, Normanby Road, Clayton 3168, Victoria, Australia

In zirconia based systems, scandia-zirconia has the highest conductivity but it deteriorates with time. However, the conductivity of fully stabilized yttria-zirconia changes little with time. Conductivity measurements (both 4 probe dc and impedance) have been combined with XRD and microstructural studies to understand the time dependent conductivity behaviour in the ternary system yttria scandia-zirconia. Nine compositions with different Y/Sc ratio (Y203+Sc203 = 8mol%) prepared by coprecipitation were investigated. In the scandia rich compositions (showing higher change in conductivity), the t'-phase, formed by diffusionless transformation from the sintering temperature at which it has a cubic symmetry, disproportionates at 1000°C into a cubic phase with t-ZrO₂ precipitates dispersed in it. In the yttria rich compositions only the cubic phase was identified which also developed t-ZrO2 precipitates with time.

(8-SIVP-89C)

CRYSTALLINITY AND HARDNESS ENHANCEMENT IN REDUCED STABILIZED ZIRCONIA

O. Nagle and V. Pai Verneker Martin Marietta Laboratories 1450 S. Rolling Road Baltimore, MD 21227

Past attempts to look for F, F' centers in yttrium stabilized zirconia (YSI), following an analogy between electroreduction of YSL and alkali halides, have resulted only in identifying colloidal zirconium and further elastic constants were found to remain unaltered. By electroducing YSL with lower voltages and at lower temperatures, we have identified F, F' centers in reduced YSL.

Data will be presented to show that Vicker's hardness and x-ray diffraction peak intensity increase before decreasing on electro and hydrogen reduction of YSL.

Ref. 1 Nagle, D., Pai Verneker, V., and Petelin, A. Mat. Res. Bulletin (in press).

(9-SIVP-89C)

TEMPERATURE AND ORIENTATION DEPENDENCES OF THE ELASTIC MODULI OF MONOCLINIC ZrO₂, * S.-K. Chan, Z. Li, * and M. V. Nevitt, Materials Science Division, Argonne National Laboratory, Argonne, IL 60439

We have calculated the temperature-dependent Young's modulus and the shear moduli of monoclinic ZrO_2 from single-crystal elastic stiffness data derived previously from Brillouin scattering measurements (Chan, Fang, Grimsditch, Nevitt, and Robertson, 91st Annual Meeting Abstracts, p. 259). As functions of crystal orientation, we show how the elastic anisotropy varies with increasing temperature premonitory to the monoclinic-tetragonal transformation.

(11-SIVP-89C)

STRUCTURE AND STABILITY MECHANISM OF Y_2O_3 Stabilized ZrO_2 , Tingkai Li, Zhijian Shen, Zishang Ding, Dept. Mat. Sci. Eng. Zhejiang University, Hangzhou, China

The nearby and lattice structures of $2r^4$ and Y^3 in yttria stabilized zirconia using EXAFS spectroscopy and HREM for a wide range of composition have been studied and the mean intervals of 2r-0 and Y-0 are obtained. The EXAFS results confirm that Y^3 replaces $2r^4$ and oxygen vacancies are produced to maintain charge neutrality. Combining EXAFS and HREM the superstructure and charge constraint models are put forward.

(10-SIVP-89C)

APPLICATION OF A NON-CLASSICAL THEORY OF NUCLEATION TO THE ZIRCONIA PHASE TRANSFORMATIONS, R.C. Garvie, CSIRO, Division of Materials Science and Technology, Clayton, Victoria, Australia; S.-K. Chan, Argonne National Laboratory, Argonne IL.

The inversions are driven by a partially softened lattice mode of vibration. It follows that the transformation temperature of a zirconia/hafnia solid solution is an inverse, linear function of the effective cation mass which is the relationship that is observed.

Assuming that the temperature dependence of the free energy arises only from the C_{**} elastic constant, the coexistence temperature, T_{*} and the upper and lower critical temperatures, T^{*} and T_{c} can be defined; they obey the constraint; $(T_{o}-T_{c})/(T^{*}-T_{o})=3$. This expectation is fulfilled by data obtained from experiments on well defined single crystals.

(12-SIVP-89C)

DEPENDENCE OF GRAIN SIZE ON PHASE TRANSFORMATION OF MONOCLINIC Z-O, TO ORTHORHOMBIC PHASE, S.Kawasaki*, T.Yamanaka, S.Kume, Osaka Univ., Toyonaka Osaka, 560 Japan

Monoclinic zirconia, which is stable at ambient pressure and room temperature, transforms into an orthorhombic form under high pressure at about 4GPa. In-situ observation of this transformation was undertaken by using diamond anvil pressure cell with X-ray energy dispersive method. The transformation rate in the pressure range up to 10GPa was evaluated from the integrated intensity ratio of the diffraction pattern. As a result, we found that sizes of grains make effect to the threshold pressure of this transformation. The threshold pressure shifts towards higher pressure side as the grain size decreases. The detailed experimental method and result will be presented.

(13-SIVP-89C)

NEW HIGH-PRESSURE PHASE OF ZrO₂ ABOVE 35 GPa, H. Arashi*, Research Institute for Scientific Measurements, Tohoku Univ, Katahira, Sendai, Japan: T. Yagi, Institute for Solid State Physics, Univ of Tokyo, Roppongi, Tokyo, Japan: S. Akimoto, Institute for Study of the Earth's Interior, Okayama Univ, Missasa, Tottori, Japan: Y. Kudoh, Geophysical Laboratory, Carnegie Institute of Washington, Washington D.C., U.S.A.

Phase transformation of pure ZrO₂ at high pressure up to 60 GPa were investigated by using X-ray diffraction and micro-Raman scattering methods. New phase transformation at 35 GPa was observed for the first time. The experimental results are reported and the candidate space groups for the newly found high-pressure phase are discussed.

(15-SIVP-89C)

TRANSFORMATION PLASTICITY AND TRANSFORMATION TOUGHENING OF ZIRCONIA-CONTAINING COMPOSITES, P.E.Reyes-Morel*, Comisión Chilena de Energía Nuclear, Santiago Chile; I-Wei Chen, University of Michigan, Ann Arbor, MI 48109-2136.

Transformation plasticity in stabilized zirconia due to the t-to-m transformation has been studied and the effects of the stress state recognized. Application of a yield criterion based on both shear and dilatation effects correlates deformation data from tension, compression, bending and indentation(1). In composites, the stress tensor is also modified by residual stresses due to mismatch in the thermal expansion coefficients between matrix and particles. Different zirconia-containing ceramic have been produced and mechanically tested to evaluate and model the effects of transformability by varying particle size, composition of the dispersed phase, testing and sintering temp-eratures, volumetric fraction of the second phase and matrix thermal expansion. (1) I-Wei Chen and P.E. Reyes-Morel, J.Am.Cer.Soc. 69 (3) 181-189 (1986).

(14-SIVP-89C)

STABLE AND METASTABLE PHASE RELATIONSHIPS IN THE SYSTEM ZrO_-ErO_ , *M.YASHIMA,M.YOSHIMURA N.ISHIZAWA,T.NOMA and S.SŌMIYA, Research Laboratory of Engineering Materials,Tokyo Institute of Technology,Yokohama,Japan.

Stable and metastable phase relationships in the system ZrO2-ErO, 5 were investigated using homogeneous samples prepared by rapid quenching of melts. The rapidly quenched samples were annealed in air 48 hrs at 1700°C or for 8 months at 1300°C. Two tetragonal phases (tand t'-phase) formed at 1700°C and t- and c-phases formed at 1300°C. The two phase regions of tetragonal and cubic phases were clarified to be from 4 to 10 mol. % at 1700°C and from 2.8 to 15 mol. % at 1300°C, which were larger than those in the literatures. The transformation behaviors of the metastable tetragonal phases in rapidly quenched samples were investigated using TMA or by grinding and crushing in a B,C mortar or by hydrothermal treatments(200°C,100MPa). Their transformability corresponds mainly to their tetragonality (axial ratio c/a).

(16-SIVP-89C)

SURFACE GRINDING INDUCED PHASE TRANSFORMATION AND RESIDUAL STRESS IN Al₂O₃-ZrO₂ COMPOSITE, G. Feng, Y. Li, Y. Chen, W.E. Mayo and W. Roger Cannon*, Department of Material Science, Rutgers University, P.O. Box 909, Piscataway, NJ 08855-0909.

Residual stresses resulting from surface grinding of Al₂O₃-ZrO₂ composites were measured. It was found that the residual stresses on ground surface increased with severity of grinding condition and were proportional to the percentage of ZrO₂ phase transformation. Parallel to the experimental work, a computer simulation model was developed to calculate the stress fields in the sample resulting from the forces of grinding and the phase transformation triggered by grinding stresses.

(17-SIVP-89C)

PHASE TRANSFORMATION BEHAVIORS Or Ce-TZP CERANICS UNDER STRESS, f. Lluang*, Z. Q. Zeng, B. Ding, L. L. Zheng, Tsingnua University, Dept. of Material Science and Eng., Leijing, China, 100084

The relationship among stress-strainphase transformation in Ce-FZP with various CeO2 contents and different sintering processes were investigated. The results snowed that yielding nnenomenon and t to m-2r02 phase transformation occurred sigultaneously under stress for Ce-TZP specimens containing 10 molx CeO2 and sintering at 1350-1500°C. And remnant plastic deformation of specimens could be recovered as heating deformed Ce-TZP specimens due to m to t-ZrJ2 reversible transition. It was found that plastic deformation at low temperature and brittle fracture at high temperature took place because critical phase transformation stress increased with increasing temperature.

(18-SIVP-89C)

FORMULA AND MECHANISM OF ZIRCONIA TRANSFORMATION TOUGHENING, Tingkai Li and Zishang Ding, Dept. Mat. Sci.Eng. Zhejiang University, Hangzhou, China

Based on analysis of the transformation thermodynamics and dynamics of zirconia and considering the contribution of nucleating potential barries to transformation toughening, the mechanism of zirconia transformation toughening is studied and a new transformation toughening formula is derived. The experimental results can be interpreted by this new model. Under special conditions the formula can be transformed into the equation acquired by predecessors.

(19-SIVP-89C)

PROPERTIES OF STRESS+INDUCED ZrO2
TRANSFORMATION, Tingkai Li, Youwen Wang
and Zishang Ding, Dept. Mat. Sci. Eng.
Zhejiang University, Hangzhou, China

The stress-induced transformation of Y203 metastable zirconia powder, the effective transformable volume fraction and the volume fraction and width of transformed ZrO2(t) in the cut and fractured surface have been measu red by X-ray diffraction. Sdudies of HREM on transformation process of ZrO2(t) and measurement of size of the ZrO2 transformation zone at crack tip have been made. It is found that there exist metastable ZrO2(t) which transformation are controlled by energy barrier forming nucleation in unconstrained condition in ZTC. The transformation of the 2r02(t) grains electively take place around defaect.

(20-SIVP-89C)

IN SITU OBSERVATION OF STRUCTURAL CHANGES OF 2.5MOL% Y-TZP BY X-RAY DIFFRACTION,Y.Kitano*,Y.Mori and A.Ishitani, Toray Research Center,Otsu,Shiga,520 JAPAN;T.Masaki and H.Kuwashima,Toray Industries, Inc.,Otsu,Shiga,520 JAPAN

Tetragonal to monoclinic phase transformation behaviour of tetragonal zirconia polycrystal containing 2.5 mol% yttria was examined by in situ X-ray diffraction. Structural and morphological changes by temperature-induced transformation were discussed in relation to surface transformation by low temperature aging and mechanical stress-induced martensitic phase transformation associated with tensile, bending and compression tests.

(21-SIVP-89C)

FABRICATION OF ZIRCONIA CEREMICS WITHOUT BINDERS- A. J. Hartshorn*, Z-TECH Pty Ltd., Division of ICI Australia, Newsom Street, Ascot Vale, Victoria 3032, Australia; S. Aruliah, Z-TECH Pty Ltd., Division of ICI Australia, Newsom Street, Ascot Vale, Victoria 3032, Australia; E. R. Caeser, CSIRO Division of Mineral Products, PO Box 124, Port Melbourne, Victoria 3207, Australia

Binders and other organic additives are added to ceramic powders to increase the strength of the green body. Using 3 mole% yttria doped Zirconia (Y-TZP) as a model powder, our investigations have shown that control of the green body uniformity and powder particle size, can give high green strength without a binder. The green bodies can be machined and because no binder burnout is required large parts can be produced with short kiln residence times.

(23-SIVP-89C)

TZP CERAMICS PREPARED FROM POWDERS DERIVED FROM EUDIALYTE, J.S. Damtoft, Aalborg Portland, DK-9100, Denmark; J. Engell*, IMI Technical University of Denmark, DK-2800, Denmark; J. Frederiksen, A/S Carl Nielsen, P.O. Box 1759, DK-2300, Denmark.

Different ceria stabilized TZP ceramics have been prepared from powders produced from sulphate solutions by a co-precipitation/calcination route. The use of both commercial chemicals and precursors derived from eudialyte have been investigated. Eudialyte is an acid soluble Zr-Y-REE-Nb-Ta-silicate occurring in a major deposit in South Greenland. Except for a nontrivial SO3 content the powders produced have many similarities with chloride-TZP powders. derived commercial Mechanical properties for the TZP ceramics prepared are reported and compared to data for reference samples made from commercial powders.

(22-SIVP-89C)

MICROSTRUCTURE & DYNAMIC BEHAVIOUR OF PZT-J. R. Sellar*, Z-TECH Pty Ltd., Division of ICI Australia, Newsom Street, Ascot Vale, Victoria 3032, Australia; L. A. Bursill, School of Physics, University of Melbourne, Parkville, Victoria 3052, Australia; Peng Ju Lin, School of Physics, University of Melbourne, Parkville, Victoria 3052, Australia

High-resolution electron microscopy has been undertaken to obtain images of PZT (lead zirconate titanate) made from Z-TECH EF SUPER grade zirconia powder, with varying amounts of nickel niobate additive. Under favourable conditions, the 400 kv accelerating voltage of the JEOL 4000EX electron microscope permits ultrahigh resolution of fragments of this material, allowing a wide variety of microstructure and behaviour to be observed. These include the gross morphology, domain structure and twinning of small grains and phase analysis of crystals.

(24-SIVP-89C)

PREPARATION AND SINTERING OF NIOBIA DOPED ZIRCONIA, D. E. Garcia, C. S. Oye and E. Longo, UFSCar, SP BRAZIL: J. A. Varela, Instituto de Quimica UNESP, SP BRAZIL

A non-conventional process was developed to obtain niobia-zirconia powder from freshly precipitated hydrous zirconia and niobiumammonium oxalate. Zirconia powders containing 0 to 16.5 mol% of niobia were prepared and calcined at temperatures from 500 to 1000 °C. The products were identified by X-ray diffraction and characterized by BET and SEM. Zirconia powders containing more than 12.0 mol% Nb205 showed single orthorhombic phase while this phase always coexisted with monoclinic phase in products that contained less than 12.0 mol niobia. Sintered bodies at 1200 to 1500°C were characterized by SEM. The densification and microstructure of undoped and niobia doped zirconia are discussed.

(25-SIVP-89C)

PRODUCTION OF HIGH PURITY ZIRCONIA, M.R. Houchin, D.H. Jenkins and H.N. Sinha*, CSIRO Division of Mineral Products, P.O. Box 124, Port Melbourne, Victoria 3207, Australia.

Australia produces over 55% of the world supply of zircon. Lower purity grades of zirconia (and zircon) have traditionally been used for refractories and ceramic colours and enamels. Value-added, high purity zirconia is finding a growing market in electronic and engineering (high technology) ceramics. This paper discusses aspects of hydrometalurgical processes for extracting high purity zirconia from zircon to produce powders suitable for ceramic fabrication.

(27-SIVP-89C)

DEVELOPMENT OF ZIRCONIA TOUGHENED CERAMICS, D. Ghosh, J. Jacobs and S. Das Gupta, The Electrofuel Mfg. Co. Ltd., Toronto, Canada.

Zirconia toughened ceramics, including partially stabilized zirconia (PSZ) and zirconia toughened alumina (ZTA), were produced by colloidal processing of commercial powders. Depending on the application in mind, properties such as hardness, toughness, thermal shock resistivity etc. were optimized through composition and processing modifications. The material properties were correlated with microstructural and phase analysis.

(26-SIVP-89C)

SINTERING OF CHROMIA-DOPED ZIRCONIA, G.R.Doughty, National Research Council of Canada, Atlantic Research Laboratory, Halifax, Nova Scotia, Canada.

An investigation has been made of the effects of minor additions of chromium oxide on the densification of zirconia in different oxygen partial pressures. The types of materials studied include unstabilized, partially stabilized and fully stabilized zirconia. Chromium oxide additions of up to 5.0 mol.% were made and densification was monitored in a controlled atmosphere dilatometer using CO-CO2-Ar gas mixtures to control the oxygen partial pressure during sintering. It has been found that chromium oxide acts as a densification aid to zirconia at low oxygen partial pressures but not in air. The differences in densification behaviour can be correlated with other properties determined by SEM and XRD; this suggests that there is an atmosphere dependent solid solubility of chromium i.n. in zirconia which alters defect concentrations and hence densification rates.

(?8-SIVP-89C)

CHARACTERIZATION OF Y-TZP POWDERS PREPARED FROM THE SPHERICAL PRECURSOR. T.Kaga*, T.Kato.Y.Kimura,M.Obitu,Central Research Lab., Nissan Chemical Industry,Ltd.,Funabashi-shi,Chiba 274,Japan

An aqueous colloidal suspension of X-ray monoclinic ZrO_2 was prepared by hydrolysis of $ZrOCl_2$ solution. The prepicitates were spherical in shape and composed of aggregation of the primary particles. The secondary particles maintained their spherical shape after calcination with 3mol% Y_2O_3 dopant to Y-TZP powder, although week agglomerates occurred. Calcination and following wet-milling conditions were investigated to make a balance between sinterability and moldability for various forming methods respectively. Correlation of sintering data and compaction behavior with powder characteristics including the particle shape was discussed.

(29-SIVP-89C)

STUDIES OF PREPARATION AND SINTERING OF DIRCONIA, Chen-Feng Kao and Tsu-Meng Fueng, Dept of Chemical Engineering, National Chung Kung University, Tainan, Taiwan

The CaO- and Y_2O_3 - stabilized ZrO_2 powders were prepared by a coprecipitating method and then forming and sintering steps. The volume fraction of tetragonal 2rO2 increased with an increase of pH values. Grain size decreased and sintering density increased with the increase of pH values. The powder washed with alcohol had a smaller grain size and was more sinterable than that washed with water. 2rO2+6 mol% Y_2O_3 powder prepared from reverse strike method can be obtained of 100% tetragonal phase when that powder was sintered at1500°C for 3 hours but that prepared from direct strike method only contains 68% of tetragonal phase. ZrO2-6 mol% CaO powder prepared from reverse strike method can be obtained of 100% tetragonal phase when that was sintered at 1200°C.

(31-SIVP-89C)

STABILIZATION OF ZIRCONIA IN CALCIUM ALUMINATE REFRACTORY MATRICES, J.L. Mendoza. Department of Ceramic Engineering, University of MO-Rolla, Rolla, MO 65401.

Calcium aluminate cements were used to stabilize monoclinic zirconias. When the calcium aluminates react to form higher alumina compounds there is a liberation of calcia which diffuses into the zirconia crystal structure promoting stabilization. Effects of processing variables including particle size distribution and purity of ZrO₂ and firing temperature were studied. Marked differences were noted in the effects of aluminate chemistry on the sinterability of the zirconia.

(30-SIVP-89C)

PREPARATION OF FINE AL₂O₃-Y₂O₃-ZrO₂ POWDERS BY HYDROTHERMAL PRECIPITATION METHOD, S. Somiya*, Nishi-Tokyo Univ, Tokyo, Japan; M. Yoshimura, Tokyo Inst. Tech, Yokohama, Japan; K. Hishinuma, T. Kumaki, Z. Nakai, T. Akiba and Y. Suwa, Chichibu Cement Co, Ltd., Kumaqaya, Japan.

We synthesized $\rm Al_2O_3 - Y_2O_3 - ZrO_2$ powders by homogeneous precipitation under hydrothermal condition. Mixed solutions of $\rm ZroCl_2$, $\rm YCl_3$, $\rm AlCl_3$ and urea were treated under hydrothermal condition at 220°C for 10 hours in $\rm Zr-lined$ autoclave. During hydrothermal treatment, these solutions were stirred at 500 rpm. They were washed with distilled water and ethanol by centrifugation to remove Cl and $\rm NH_4$ ions. The powders obtained consisted of c-ZrO_2 and boehmite. Particle size was extremely fine as expressed in terms of 10nm powder of zirconia was homogeneously mixed with boehmite. Boehmite was transformed into $\rm \alpha - Al_2O_3$ by calcination at 1200°C. Highly dense composite with a homogeneous microstructure was obtained.

(32-SIVP-89C)

EVALUATION OF ZIRCONIA CERAMICS STABILIZED WITH CALCIUM ALUMINATE CEMENTS, J.L. Mendoza, Department of Ceramic Engineering, University of Missouri-Rolla, Rolla, MO 65401.

Monoclinic zirconias and calcium aluminate powders were mixed in the proportion to produce calcium hexa-aluminate and tetragonal zirconia containing refractory matrices. Evaluation of some engineering properties such as thermal expansion, thermal shock and fracture toughness as well as mineralogical and microstructure analyses are included.

(33-SIVP-89C)

COARSENING KINETICS IN Mg (Ca, Ti, Y) PSZ's, C.A. Bateman*, M.R. Notis, C.E. Lyman, Materials Science and Engineering, Lehigh University, Whitaker Laboratory, #5, Bethlehem, PA 18015

The strength of PSZ materials depends greatly upon the size and distribution of the metastable tetragonal precipitates and yet, although qualitative studies have been performed, there is little quantitative data on coarsening in PSZ systems. The coarsening kinetics of tetragonal precipitates in a 9 Mg PSZ and a 9 Mg PSZ with additions of calcia, titania, or yttria at the 2 mol% level have been measured in the TEM. The addition of the third oxide, even at the relatively low level used, has a marked effect on the coarsening rate of the precipitates. The reasons for the observed differences between the different systems will be discussed in terms of precipitate volume fraction, defect chemistry, and cationic radii.

(35-SIVP-89C)

PROPERTIES OF YTTRIA-STABILIZED ZIRCONIA PREPARED BY OXALATE METHOD IN ETHANOL SOLUTION, Guo Gongyi, Dept of Materials Sci/Eng, Shanghai Jiao Tong University, Shanghai, China: Chen Yuli, Dept of Themistry and Chemical Eng, Shanghai Univ/Technology, Shanghai, China.

The almost full tetragonal zirconia powder and sintered body which are stabilized with yttria at a low mole fraction at room temperature can be prepared by oxalate method in ethanol solution. The powder only contains weak agglomerates and shows very narrow particle size distribution range. In general, the cumulative weight percentage of the particles from 0.2 to 1µm can be as high as 75.9% and the weight percentage of particles with an average particle size of some 0.4 mm may constitute 33% of the powder product. It is possible to prepare over 98% theoretical density sintered body by simple cold pressing followed by pressureless sintering in air at temperatures as low as 1300°C. The bending strength and Vickers hardness of the sintered body were 570 MPa and 11 GPa, respectively.

(34-SIVP-89C)

MICROSTRUCTURAL CHANGES DURING ISOTHERMAL HEAT TREATMENT OF TETRAGONAL ZrO2-Gd2O3 CERAMICS

D. K. Leung*, C. J. Chan, I. Nettleship, F. F. Lange, and M. Rühle, Materials Department, University of California, Santa Barbara, CA 93106

Polycrystalline tetragonal zirconia ceramics containing 3 mol% Gd₂O₃ exhibit a very fine grain size after extended heat treatment at 1400°C. This is analogous to TZP ceramics containing Y₂O₃. Analytical electron microscopy has been used to study the phase evolution and variation in microchemistry. The correlation between phase partitioning and grain growth is discussed.

(36-SIVP-89C)

GRAIN GROWTH CONTROL IN ZIRCONIA POLYCRYSTALS, S.L. Huang* and I-Wei Chen, Department of Materials Science and Engineering, University of Michigan, Ann Arbor, MI 48109-2136. (313) 763-6661.

Grain size control is an integral part of the zirconia science and technology, both for structural and for electrochemical appplications. We have systematically investigated the solute effects on grain growth and found that a fine-grain polycrystal can be achieved when solute segregation occurs on the grain boundary. A consistent picture is now obtained in terms of ionic size and ionic charge. This picture will be exemplified by the grain growth behaviors in a large number of tetragonal and cubic zirconia alloys.

"Processing and Microstructure Control"

Session Chair: Fred F. Lang, Dept. of Materials, University of California, Santa Barbara, CA 93106

8:00-8:20 a.m.-(16-SIV-89C)

DENSIFICATION BEHAVIOR OF SINGLE CRYSTAL AND POLYCRYSTALLINE SPHERICAL PARTICLES OF ZIRCONIA, E.B. Slamovich*, F.F. Lange, Department of Materials, University of California, Santa Barbara, CA 93106

Polydispersed spheres of zirconia were produced via electrostatic atomization and pyrolysis of mixed zirconium acetate-yttrium acetate precursors. Different compositions in the ZrO2 rich portion of the ZrO2-Y2O3 binary system allowed the production of either single crystal (0 and 10 mole % Y2O3) or polycrystalline (3 mole % Y2O3) zirconia spheres, of similar size distribution, for densification studies. Powders of the either single crystal or polycrystalline particles exhibited contrasting densification behavior, powder compacts composed of polycrystailine particles attaining significantly higher endpoint densities than their single crystal counterparts. Observations suggest that the substructure of the polycrystalline particles prevents the formation of metastable particle networks which are characteristic of the microstructural development of single crystal powder compacts. The role of grain growth within the polycrystalline particles is discussed in the context of the above results.

8:20-8:40 g.m.—(17-SIV-89C)

SINTERING OF NANO-SCALE ZrO2-Y203 CERAMICS, G.S.A.M. Theunissen, A.J.A. Winnubst,A.J.Burggraaf, University of Twente, Faculty of Chemical Technology, P.O. Box 217, 7500 AE Enschede, The Netherlands.

A dense ceramic of Y-TZP (3 mol% Y2O3) with a grain size of 50 nm is obtained after sintering at 1320 K during 6.5 hours. Grain boundary sliding is an important mechanism during densification and plastic deformation. In potential this ceramic shows good superplastic behaviour and low temperature deformability.

The materials are prepared by a gelprecipitation technique. This results in a powderstructure containing few aggregates and weak agglomerates.

Densification behaviour, pore morphology and grain growth is followed during the sintering of this powder.

Some values for the fracture toughness and bending strength of these ceramics will be given.

8:40-9:00 a.m.-(18-SIV-89C)

ALCOHOL INTERACTION WITH ZIRCONIA POWDERS. M. S. Kaliszewski and A. H. Heuer, Department of Materials Science and Engineering, Case Western Reserve University, Cleveland, OH.

Alcohol washing of Zr0, powders is a powerful method for controlling the state of agglomeration of fine sinterable powders. The interaction between alcohol and the Zr0, powder surfaces has been studied using FTIR and a model explaining the beneficial effects of alcohol in producing soft agglomerates is proposed.

9:00-9:20 s.m.-(19-SIV-89C)

GRAIN GROWTH OF TETRAGONAL ZIRCONIA I. Nettleship*, D.K. Leung, C.J. Chan, F.F. Lange and M. Rühle, Materials Dept., University of California, Santa Barbara 93106.

Solid solutions derived from aqueous zirconium acetate and metal nitrates have been used to study grain growth of tetragonal zirconia in binary oxide systems. The effects of substituting cations of differing valency and ion size were examined.

Fine grained tetragonal zirconia was observed in all the systems of the type ZrO₂-M₂O₃ that were investigated. Preliminary observations suggest these materials are in the cubic-tetragonal two phase region. In each case grain growth of the tetragonal phase at 1400°C was slower than for the ZrO₂-CeO₂ system.

9:20-9:40 a.m.-(20-SIV-89C)

EVALUATION OF GRAIN SIZE AND YTTRIA SEGREGATION EFFECTS IN TZP VIA ELECTRICAL MEASUREMENTS, R. Gerhardt*, L. Braun and W. R. Cannon, Dept. of Ceramics, Rutgers University, Piscataway, NJ

Large grain sizes and long sintering times are known to result in significant changes to the mechanical behavior of TZP. Since electrical properties have been shown to be sensitive to microstructural changes, we decided to employ a.c. electrical measurements as a non-destructive technique which could provide some information regarding grain size and segregation effects in TZP. Samples heat treated between 1200 C and 1600 C at soaking times of 1, 5, 10 and 20 hr were evaluated over the frequency range 10 Hz-10MHz at various temperatures. results are strongly dependent upon the heat treatment and suggest that grain size and yttria segregation play a very important role in determining the electrical behavior. Microstructural and microchemical results obtained by analytical electron microscopy support these conclusions. Correlation with the mechanical properties will also be attempted.

10:00-10:20 a.m.-(22-SIV-89C)

DYNAMIC COMPACTION OF STABILIZED ZIRCONIA, N.J. Kiwiet, J. Schoonman, Laboratory for Inorganic Chemistry, Delft University of Technology, P.O. Box 5045, 2600 AG Delft, the Netherlands; A.C. van der Steen, H.H. Kodde, PML-TNO, P.O. Box 45, 2280 AA, Rijswijk, the Netherlands

Powders of Yttria Stabilized Zirconia (YSZ) are densified through dynamic compaction. The microstructure and electrical properties of the compacted material are investigated by SEM and impedance spectroscopy. The bulk ionic conductivity and grain boundary polarization phenomena are studied under a constant partial pressure of oxygen, as a function of temperature (400 - 800 C), over the frequency range of 10⁻⁴ and 65 kHz The data for boundary grain polarization compared to data obtained on pressed and sintered YSZ.

9:40-10:00 a.m.-(21-SIV-89C)

MICROSTRUCTURE DEVELOPMENT IN A 9 Mg 2 Y PSZ AT 1420°C, C.A. Bateman* and M.R. Notis, Materials Science and Engineering, Lehigh University, Whitaker Laboratory, #5, Bethlehem, PA 18015.

It appears to be accepted that in Mg PSZ materials 3 variants of the disk-like tetragonal precipitates are produced and that they simply coarsen with time upon aging at 1420°C. The microstructure development in a 9 Mg 2Y PSZ alloy has been studied and the observations made are in considerable disagreement with accepted ideas. It is found that both the precipitate morphology and number of precipitate variants present vary as a function of aging time. The driving force for the microstructural development and similarities with the Mg PSZ system will be discussed.

10:20-10:40 a.m.-(23-SIV-89C)

THE INFLUENCE OF SILICATE PHASES ON THE STRUCTURE AND PROPERTIES OF Y₂O₃-ZrO₂, M.L. Mecartney, Dept. of Chem. Eng. and Mat. Sci., University of Minnesota, Minneapolis, MN 55455.

The properties of Y₂O₃-ZrO₂ ceramics can be modified by the presence of small amounts of silicate glass phases. The specific chemical composition of the amorphous grain boundary phase controls the solubility of ions and the rate of transport of ions. These glassy phases can enhance densification via liquid phase sintering, and protect the sintered component from reduction. Glass additions can be designed to scavenge Y2O3 from the ZrO2 grains, or made to have an extremely low solubility for Y2O3. Certain silicate compositions promote crystallization of zircon and mullite, while others remain amorphous. Small amounts of these silicate phases can have a tremendous influence on grain growth, both for the cubic and the tetragonal + cubic ZrO2 systems. Modification of residual stresses by these silicate phases influences the mechanical properties (especially the amount of transformation toughening), although the crack propagation path does not appear to be significantly affected. The role of specific glass compositions in controlling the structure and properties of Y2O3-ZrO2 ceramics will be detailed.

10:40-11:00 a.m. -- (24-SIV-89C)

THE SINTERING BEHAVIOR OF ZIRCONIA FIBER PRE-CURSOR IN OXIDIZING AND NON-OXIDIZING ATMOS-PHERE, S.S. Jada*, J.F. Bauer, F. D'Ovidio, N.G. Peletis, Manville Corp. R&E Center, P.O. Box 5108, Denver, CO 80217.

Pure zirconia fiber precursor has been sintered at temperatures upto 1000° C in 0_2 and No environment and the products investigated by x-ray diffraction, transmission electron microscope (TEM), SAED, DSC and thermogravimetric techniques. Crystallization occurred at 450°C yielding the pure tetragonal phase in both 02 and N2 atmospheres. Increase in sintering temperature and change in sintering media brought differences in polymorphic phase transformation and composition. The average particle diameter for N2 sintered sample is 220A and for O_2 it is 670A. DSC shows marked exotherm at 290-400°C which is attributed to residual organics; no distinct evidence of ZrO_2 phase transformation was found. Carbon contaminated zirconia precursors are resintered in air and the changes in phase composition, nucleation and grain growth will be discussed.

11:20-11:40 a.m.-(26-SIV-89C)

INVESTIGATION OF PLASMA SPRAYED ZIRCONIA ALUMINA, COATINGS, M.C. Foujanet Sainte-Catherine, J.P. Lumet, J.L. Derep, E.T.C.A., Arcueil France; F. Nardou, Laboratoire de céramiques nouvelles. Université de Limoges France.

Zirconia (with 7-8 wt% Y₂O₃) alumina powder mixtures were plasma sprayed to obtain duplex coating structures. Macrostructure (e.g. porosity, cracks, chemical and crystalline compositions) is discussed in relation to plasma spraying parameters. Examination of microstructure by transmission electron microscopy allows correlations between the typical structure of such coatings and their properties. Mechanical and thermal properties of these composite plasma sprayed coatings (e.g. Young modulus, rupture strength, thermal insulation) are essentially governed by limited areas of contact between lamaliae, pores and microcracks rather than by addition of alumina.

11:00-11:20 a.m.-(25-SIV-89C)

DEVELOPMENT OF MICROSTRUCTURE IN Si₃N₄-ZrO₂ CERAMICS, L.K.L. Falk, Department of Physics, Chalmers University of Technology and University of Göteborg, S-412 96 Göteborg, Sweden

The development of microstructure in Si₃N₄-ZrO₂(+Y₂O₃) composite ceramics has been characterized by analytical electron microscopy in combination with xray diffractometry. The ceramics were formed with 30 wt% ZrO2 powder which had been pre-reacted with 3 mol% Y₂O₃. Densification was carried out by pressureless sintering or hot-pressing at temperatures in the range 1650 to 1800 °C, and resulted in a general microstructure consisting of an Si₃N₄ matrix containing grains of tetragonal ZrO2 and Si2N2O. These ceramics contained an extremely small volume fraction of residual glass. Oxidation at 1200 °C caused a decomposition of the ZrO2 grains, which implies that N had entered the ZrO₂ lattice during sintering. This decomposition introduced internal stresses in the material, which caused cavitation and cracking in a zone below the oxide scale.

"Oxygen Sensors and Electrochemical Catalysis"

Session Chair: Wayne L. Worrell, University of Pennsylvania, Philadelphia, PA 19104

1:00-1:40 p.m.-(27-SIV-89C)

TETRAGONAL ZIRCONIA FOR LOW-TEMPERATURE OXYGEN SENSORS, W.J.F. Weppner, Max-Planck-Institut fur Festkorperforschung, Stuttgart, West Germany

Tetragonal zirconia has not only more favorable thermomechanical properties but also superior electrical properties than cubic zirconia. Gas-impermeable polycrystalline samples of tetragonal zirconia have been prepared in various dopant concentrations with grain sizes less than 0.3 microns to prevent a phase transformation into the monoclinic structure at low temperatures without a serious effect on the conductivity. Potentiometric-type oxygen sensors show Nernstian behaviour at temperatures as low as 150°C. Amperometrictype diffusion limited oxygen sensors are applicable at even lower temperatures, where bulk transport in the electrolyte is the rate-controlling process. The electronic conductivity of tetragonal zirconia may also be employed for oxygen sensing. Application of thin film electrolytes is favorable. Mechanically prepared small diffusion holes may be replaced by oxide bulk diffusion barriers.

1:40-2:00 p.m.-(28-SIV-89C)

DEVELOPMENT OF NEW EXTENDED-LIFE ZIRCONIA SENSORS, Qingguo Liu, University of Science and Technology Beijing 100083, PRC and Wayne L. Worrell, University of Pennsylvania, Philadelphia, PA 19104 USA

New extended-life sensors have been developed using fully-stabilized zirconiayttria electrolytes to minimize the shortcircuit electronic conductivity exhibited by partially-stabilized zirconia-tube sensors. An inexpensive fabrication technique is used to eliminate conventional sintering processes and the thermal-shock problems associated with fully-stabilized electrolytes. The metal/metal oxide reference electrode is completely encased by the isostatically pressed zirconia electrolyte. Iron and steel melts do not penetrate the porous electrolyte, and reliable results are obtained over time periods as long as ten hours at 1600°C. Another new and improved design for extended-life oxygen sensors is also described.

2:00-2:20 p.m.-(29-SIV-89C)

ELECTRONIC CONDUCTIVITY AND THERMAL SHOCK STABILITY OF MAGNESIA PARTIALLY-STABILIZED ZIRCONIA, Shengli An, Tuping Zhow, Weijiang Wu, Qingguo Liu, University of Science and Technology, Beijing 100083, PRC

The effects of magnesia content and impurity concentrations (Al₂O₃, TiO₂) on the electronic conductivity of magnesia partially-stabilized zirconia (MgO-PSZ) have been investivgated. A polarization technique is used to develop zirconiaelectrolyte tubes for measuring very low oxygen concentrations in iron and steel melts. A new X-ray diffraction method has been developed to measure quantitatively the proportions of monoclinic, tetragonal and cubic phases in MgO-PSZ. A dilatometric technique is used to determine the expansion characteristics of MgO-PSZ tubes which were sintered at different temperatures and heattreated with different temperature profiles. The relationship of thermal-shock resistance with the expansion characteristics and phase proportions are discussed.

2:20-2:40 p.m.—(30-SIV-89C)

RATES OF DESORPTION OF OXYGEN FROM CALCIA-STABILIZED ZIRCONIA, Shixue Dou, University of New South Wales, Kensington, Australia; Charles R. Masson, National Research Council, Halifax, Canada; Philip D. Pacey*, Dalhousie University, Halifax, Canada.

Samples of calcia-stabilized zirconia were equilibrated with oxygen at 50 Pa to 100 kPa and 1250 K to 1600 K. The gas was then pumped out and the rate of oxygen desorption was measured. The diffusion coefficient of oxygen in the ceramic was inversely proportional to the content of iron impurities. The observations were interpreted in terms of a mechanism in which dissolved oxygen was effectively trapped by these iron impurities. This trapping leads to sluggishness in the performance of zirconia oxygen sensors. Reduction in the iron impurity allows substantially improved sensor response times. C.R. Masson, P.D. Pacey, S. Dou, Solid electrolite for oxygen sensor, U.S. Patent 4,749,466(1988).

2:40-3:20 p.m.-(31-SIV-89C)

NON-FARADAIC ELECTROCHEMICAL MODIFICATION OF CATALYTIC ACTIVITY IN ZIRCONIA-ELECTROLYTE CELLS, C.G. Vayenas, Institute of Chemical Engineering and High Temperature Chemical Processes, University of Patras Patras 26110, Greece

The catalytic activity and selectivity of metal catalysts used as electrodes in high temperature stabilized zirconia cells can be altered dramatically and in a reversible manner. This is accomplished by electrochemically supplying oxygen anions onto catalytic surfaces via polarized metalzirconia interfaces. Oxygen anions, forced electrochemically to adsorb on the metal catalyst surface, alter the catalyst work function in a predictable way and lead to reaction rate increases as high as 5000% Changes in capalytic rates typically exceed the rate of 0 transport to or from the catalyst surface by 102-3 105. Significant changes in product selectivity have been also observed. The case of several catalytic reactions in which this new phenomenon has been observed is presented, and the origin of the phenomenon is dis-

California Pavilon C Anaheim Hilton Thursday Afternoon • November 2

"Defects and Their Role in Ionic Conductivity"

Session Chair: Arturo Dominguez-Rodriquez, Universidad de Sevilla, Sevilla, Spain

3:20-3:40 p.m.-(32-SIV-89C)

INVESTIGATION OF THE DEFECT STRUCTURE IN ZrO₂:Y₂O₃ WITH IONIC CONDUCTIVITY AND DIELECTRIC LOSS, S.Ling and M.P.Anderson, Exxon Research & Engineering Co., Annandale, NJ 08801

 $\rm ZrO_2$ samples doped with 1 to 5.8 mole $\rm \%~Y_2O_3$ were pressed and sintered. Ionic conductivity and dielectric loss of the samples were measured with a.c. complex impedance and thermally stimulated depolarization techniques respectively. Defect concentrations and energies were determined from these measurements. In particular, the different behaviors exhibited by $\rm ZrO_2$ of various phases were examined. An atomistic model involving yttrium-oxygen vacancy complex is presented to account for the observations.

3:40-4:00 p.m.-(33-SIV-89C)

LOW TEMPERATURE IONIC CONDUCTIVITY OF YTTRIA STABILIZED ZRO2 SINGLE CRYSTALS WITH DIFFERENT SOLUTE CONCENTRATIONS, J.D. Solier, A. Dominguez-Rodriguez and A.H. Heuer, Dept of Materials Sci/Eng, Case Western Reserve University, Cleveland, OH 44106

Ionic conductivity and dielectric permitivity were measured from room temperature to 900°C in fully stabilized ZrO2 with different concentrations of Yttri single crystals using a four-probe complex impedance spectroscopy method and a four-probe direct current electrical conductivity method. We separated the long range ionic diffusion (σ_{dc}) correlated with the migration of oxygen vacancies from the permanent dipole reorientation or other motions that do not involve displacement of mobile charge carriers over long distance. We observe a gradual transition between low temperature (clusters of defects) and high temperature (vacancies free) activation energies and this transition increase in temperature as well as the activation energies values when the cationic concentration increase.

4:00-4:20 p.m.-(34-SIV-89C)

OXYGEN VACANCY TRAPPING AND HOPPING IN TETRAGONAL AND CUBIC ZIRCONIA:A MICROSCOPIC STUDY BY PAC SPECTROSCOPY, H. T. Su, H. Jaeger, H. Fuchs, A. G. McKale, and John A. Gardner*. Department of Physics, Oregon State University, Corvallis, OR 97331; J. A. Sommers and D. P. Carter, Teledyne Wah Chang Albany, Albany, OR 97321

We have used Perturbed Angular Correlation (PAC) spectroscopy to determine the concentration and hopping barrier energy of free vacancies as well as the trapping properties of vacancies near a divalent impurity. We have examined both tetragonal and cubic zirconia with varying concentrations of trivalent stabilizers. Such measurements yield bulk oxygen diffusivities more directly than macroscopic techniques and can often be used in complex materials where bulk measurements can give only average diffusivities.

4:40-5:00 p.m.-(36-SIV-89C)

A COMPUTER SIMULATION STUDY OF DEFECTS AND ORDERED PHASES IN THE CaO-ZrO₂ SYSTEM, Anurag Dwivedi and A. N. Cormack, Alfred University, Alfred, NY-14802

An atomistic computer simulation technique has been used to investigate lattice and defect energies of some phases of interest in the CaO-ZrO₂ system. A potential model was developed which reproduces the crystal structures and other physical properties of ZrO₂. A notable observation is that intrinsic disorder in ZrO₂ is predicted to be of Schottky type.

On addition of CaO, for charge compensation oxygen vacancies are created; these are found to be energetically more stable at next nearest neighbour sites to the dopant Ca ion, than nearest neighbour positions.

The formation of larger clusters have been examined as well as the formation of the ordered phases $CaZr_4O_9$ and $CaZrO_3$. Energy minimisation techniques were used to predict a crystal structure for $CaZr_4O_9$ because the crystal structure of this phase has not vet been reported in the literature. There is found to be a very small driving force for the formation of $CaZr_4O_9$ which explains the observed sluggishness in the development of this phase.

4:20-4:40 p.m.—(35-SIV-89C)

EPR STUDY OF DEFECT STABILITY IN X-IRRADIATED YTTRIA STABILIZED ZIRCONIA, C.B. Axxoni and A. Paleari, Dipartimento di Fisica A. Volta Dell'Universitta di Pavia, via Bassi 6, 27100 Pavia, Italy

The stability of the oxygen vacancy EPR defect induced by X-ray in Yttria stabilized Zirconia is studied by using isochronal and isothermal pulsed annealings. The signal, almost unchanged after 4 months at room temperature, vanishes at 300°C, having a half-life of 10 minutes at 200°C. Other authors observed a lower stability, probably for the presence of competitive impurity traps. If this is the case, the defect stability in reduced samples suggest an inhibiting role of hydrogen in the trapping processes at impurity sites.

5:00-5:20 p.m.-(37-SIV-89C)

ELECTRONIC STRUCTURE OF PHASE STABILIZING DOPANTS IN ZRO2:EXPERIMENT AND THEORY, R. H. French*1, D. E. Ellis2, F. S. Ohuchi1, V. C. Long1, W. Y. Ching2, D. J. Lam3 1, DuPont Co, Central Research, Wilmington DE, 19880.2. Physics Dept. Northwestern Univ, Evanston IL, 60201.3. Argonne Nat'l Labs, Argonne IL, 60439.

The phase stabilizing dopants Y and Ca have been studied as a function of concentration in cubic ZrO2 using vacuum ultraviolet and valence band photoemission spectroscopy coupled with self-consistent embedded-cluster electronic structure calculations. The band gap energy of cubic ZrO2 (5.3 eV expt.) is unaffected by the presence of Ca or Y stabilizers. The Ca2+ and Y3+ valence bands reside below the O 2s lower valence band, while their conduction bands are degenerate with the Zr 4d conduction bands. There is experimental evidence of the presence of Zr 4d valence states which suggest Zr in a 2+ oxidation state. Electronic structure calculations of cubic ZrO2 with Ca or Y as nearest or second nearest neighbors to the oxygen vacancy have been performed to understand the role of stabilizers in the electronic structure and total energies of ZrO2.

Thursday Afternoon • November 2 Poster Session — 5:20-7:00 p.m.

"Mechanical Properties/Microstructural Correlations"

Session Chair: Keith J. Bowman, School of Materials Engineering, Purdue University, West Lafayette, IN 47907

(37-SIVP-89C)

EFFECT OF Al₂O₂ ADDITION ON MECHANICAL PROPERTIES AND MICROSTRUCTURE OF Ce-TZP, S.K.Chung, K.W.Ahn⁴, CERATEC (Korea New Ceramics Tech. Lab.), 417-1, Duksungri, Yongin, Korea.

Effects of various CeO contents on the mechanical properties and microstructure of CeTZP were studied.

The results show that fracture toughness was decreased, because crack propagates from transgranular to intergranular under stress with increasing CeO₂ contents.

increasing CeO₂ contents.

The 12-16 mol% CeO₂-doped ZrO₂ containing 10-40 wt% Al₂O₃ were prepared by die pressing, cold isostatic pressing and sintering at 1450-1650 C for 2-10 hrs in air.

The mechanical properties of the Ce-TZP/Al₂O₃

were compared to Ce-TZP.

Also, the effect of post-HIPing on Ce-TZP and Ce-TZP/Al₂O₃ will be discussed.

(38-SIVP-89C)

REINFORCEMENT OF Y₂O₃- AND CeO₂-DOPED TETRA-GONAL ZIRCONIA POLYCRYSTALS BY Al₂O₃-PLATE-LETS, K.-H. Heussner* and N. Claussen, Technical University of Hamburg-Harburg, Advanced Ceramics Group, P.O. Box 90 14 03, D-2100 Hamburg 90, Federal Republic of Germany

The effect of Al_2O_3 platelets in tetragonal zirconia polycrystals (TZP) on the mechanical properties was investigated. Composites of Y₂O₂- and CeO₂-doped ZrO₂ (Y-TZP, Ce-TZP) with up to 20°vol % platelets were fabricated by hot isostatic pressing. Microstructures of various grain sizes were produced by high temperature aging. In high strength fine grained Y-TZP the addition of platelets causes an increase in fracture toughness due to crack deflection. Platelets increase the flaw size and thus the strength decreases considerably. Platelet reinforced high toughness Ce-TZP exhibit slightly higher strength than the pure matrix which is due to modulus load transfer. The fracture toughness is lowered in these composites because inclusions decrease the process zone size in Ce-TZP.

(39-SIVP-89C)

EFFECT OF MnO AND Al₂O₃ ADDITIVES ON THE MICROSTRUCTURES AND MECHANICAL PROPERTIES OF CERIA-PARTIALLY-STABILIZED ZIRCONIA (CeO₂-TZP), J. S. Wang, D. K. Shetty and A. V. Virkar, University of Utah, Salt Lake City, UT

Effect of increasing amounts of MnO additions on the microstructures and mechanical properties of ZrO2-12 m% CeO₂ and ZrO₂ -12 m% CeO₂ -10 w% Al₂O₃ were studied. MnO suppressed grain growth in ZrO2-12 m% CeO₂, while enhancing the mechanical properties significantly (strength = 557 MPa, fracture toughness = 9.3 MPa.vm at 0.2 w% MnO). The enhanced mechanical properties were achieved despite a reduced volume fraction of the monoclinic phase on the fracture surface. In ZrO2 -12 m% CeO2 - 10 w% Al2O3, the addition of MnO suppressed the grain size of ZrO2, but promoted grain growth of Al₂O₃. Fracture toughness increased monotonically to 13.2 MPa. vm with addition of up to 2 w% MnO. However, strength was initially constant at about 600 MPa, but decreased for MnO content greater than 1.5 w%. This decrease in strength was associated with increased transformation plasticity (up to 1.2 % in four-point bending).

(40-SIVP-89C)

INFLUENCE OF ALUMINA ON THE FRACTURE BEHAVIOR OF Y-TZP S. Jill Glass and David J. Green*, Center for Advanced Materials, The Pennsylvania State University, University Park, PA 16802

Alumina (~5 vol. %) was introduced into Y-TZP by an infiltration process. This process involves introducing aluminum nitrate into a porous Y-TZP compact and is followed by decomposition of the nitrate to alumina and densification of the composite. It was found that the alumina addition led to increases in strength and fracture toughness. These changes were accompanied by a shift from intergranular to transgranular failure. The improvement in the mechanical properties will be discussed in terms of the microstructure of these materials, especially the distribution and morphology of the alumina phase. For example, the alumina particles tend to form interconnected, single crystal clusters and there is a concentration gradient of the alumina from the outer surface towards the interior of the materials.

(41-SIVP-89C)

MECHANICAL PROPERTIES OF ZTA COMPOSITES WITH NON TRANSFORMING ZIRCONIA, R. Langlois* IMRI-NRC, Bouonerville, Québec, Canada, K. Konsztowicz, ARL-NRC, Halifax, N.S., Canada.

Composite samples were obtained by colloidal filtration of ZrO_2/AL_2O_3 dense water suspensions containing 50 vol. % of solids with 5 to 30 vol% of ZrO_2 . No deflocculants were used, and the zirconia was of sub-micron size. Tetraganal form of ZrO_2 was retained after pressureless sintering at 1500°C (99% T.D.), grinding and polishing the samples.

Elastic properties, strength and fracture toughness after sintering were related to the mechanical properties of the green bodies. These data, along with the results of systematic study of dispersion properties in water suspensions suggest that toughening in ZTA composites might also originate with heterofloculation of powders, leading to formation of crack-like voids in the green bodies during casting.

(43-SIVP-89C)

THE EFFECT OF MICROSTRUCTURAL FEATURES OTHER THAN GRAIN SIZE ON THE FRACTURE TOUGHNESS OF Y-TZP, L.M. Braun *, W.R. Cannon, R.M. Anderson, Department of Ceramics, Rutgers University, Piscataway, NJ

Fracture toughness values measured on 2.5 mole % Y-TZP sintered at various temperatures for 1, 10, or 20 hours were found to depend on microstructural features other than average grain size. The heat treatment was found to influence not only the grain size, but also grain size distribution and yttria segregation. Microstructural results obtained by analytical electron microscopy suggest yttria segregation to the grain boundries. These microstructural features are more strongly dependent on sintering temperature not time. The effect of these parameters on the chevron notch fracture toughness and R-curve behavior will be discussed.

(42-SIVP-89C)

PHYSICAL AND MECHANICAL PROPERTIES OF YTTRIA-STABILIZED TETRAGONAL ZIRCONIA POLYCRYSTALS DOPED WITH LITHIA,P.E. Reyes-Morel* and R. Becerra, Comision Chilena de Energia Nuclear, Santiago, Chile.

Y203-stabilized tetragonal zirconia polycrystals (Y-TZP) containing 1.5 to 3.5 mol% yttria and 0.1 to 2.0 mol% Lithia were prepared and tested to evaluate their physical and mechanical properties. Results obtained from fracture toughness measurements, stress-strain curves and dilatometry are consistent with our knowledge of transformation plasticity, transformation toughening and auto-catalysis(1). The effects of environmental conditions were studied with relation to phase stability. The implications of microstructure, composition and presence of defects and their relation with mechanical and environmental phase stability were explored.

(1) P.E.Reyes-Morel and I-Wei Chen, "Transformation Plasticity of CeO2-Stabilized Tetragonal Zirconia Polycrystals:I, Stress Assistance and Autocatalysis", J. Am. Cer. Soc. 71(6)343-353(1988).

(44-SIVP-89C)

SURFACE MODIFICATION IN Y-TZP AND CE-TZP, J.G. Duh* and Y.S. Wu, Department of Materials Science and Engineering, National Tsing Hua University, Hsinchu, Taiwan

Ion beam treatments affect the near-surface region of ceramics, and posses the potential for changing the surface composition, stress state and microstructure. As-sputtered ZrO₂ ceramics are ion implanted with various ion source at different doses. Microstructure, hardness, fracture toughness and composition variation of the implanted ceramics are evaluated. The potential for surface modification is discussed with respect to the sputtered materials, ion implantation dose and species. The feasibility for further development will be probed.

(45-SIVP-89C)

SHAPE MEMORY EFFECT IN Ce-TZP/Al $_2$ O $_3$ COMPOSITE C. Schmid, O. Sbaizero and S. Meriani, Appl. Chem. Inst., University of Trieste, Italy.

Ce-TZP ceramics have given rise to a "second generation" of transformation toughened ceramics; they exhibit a much larger t-m process zone if compared with the classic PSZ materials. The increase of the energy dissipative, crack shielding volume is due to a stress assisted, deformation induced, reversible t-m transformation, being both phases within the metastability range of the equilibrium phase diagram. We have studied a ceramic composite made of Ce-TZP (8.5 mol% CeO2) matrix with 10 weight% alumina particles. The material showed at room temperature a reversible stress-strain curve in bending and counter-bending before fracture. Permanently bent, unbroken specimens, showed large deformation bands on the tensioned surface with a monoclinic XRD pattern whereas the opposite compresses surface was fully tetragonal. Bent specimens showed a "shape memory effect" because they underwent a full recovery by being heated above 200°C.



THE MECHANIGAL PROPERTIES OF ZTA, Tingkai Li, Zishang Ding, Dept.Mat. Sci. Eng. Zhejiang University, Hangzhou, China

The mechanical properties of ZTA ceramics have been studied. It is found that there are two suitable range in Zr02-Al203 system: Addition of Zr02 grains to Al203 matrix can toughen and strengthen alumina ceramics, and addition of Al203 to Zr02 matrix can increase Kc and G, of Zr02-Alloys. This is because that the transformation of Zr02(t) could toughen and the crack deflection caused by Al203 grains could strengthen the transformation toughening of Zr02. Controlling Y203 content in YMSZ and Al203 content we obtained ZTA ceramics with high toughness and strength.

(47-SIVP-89C)

STRENGTH ANALYSIS OF YTTRIA-STABILIZED TETRAGONAL SIRCONIA POLYCRYSTALS, K. Moguchi* and M. Gishi, Toray Research Senter, Inc., Otsu, Shiga, 520 JAPAN; T. Masaki, S. Nakayama and M. Mizusnina, Toray Industries, Inc., Otsu, Shiga 520 JAPAN

This paper describes the effects that the defects have on tensile and bend strength distributions. Tensile strength of Y-TZP was measured using the newly developed tensile testing method. Defects causing fracture vere characterized by examining the fracture surfaces of tensile and bend specimens using scanning electron microscopy. The strength distributions were analyzed by the multi-modal Weibull distribution function.

(48-SIVP-89C)

ZIRCONIA TOUGHENED COMPOSITES, M.G.Cain*and M.H.Lewis, University of Warwick, U.K.

Silicon Nitride based Zirconia toughened composites were fabricated using conventional hot pressing techniques. The material had a high density with a significant retention of tetragonal Zirconia resulting in enhanced levels of fracture toughness. The effects of Zirconia solute additive on the fracture toughness and on the retention of tetragonal Zirconia was investigated and, together with microstructural characterisation, possible toughening mechanisms were suggested.



(49-SIVP-89C)

EROSIUN OF TZP AND ZTA BY SOLID PARTICLE IMPACT, L. Zhang, Z. Y. Mao, T. K. Li and Z.J. Shen, Materials Department, Zhejiang University, Hangzhou, P. R. China

The erosion behavior of a series of TZP and ZTA was determined using SiC, Al_2O_3 , SiC₂ as erodents. The results showed that besides the conventional feature for brittle materials (erosion peak at 90°), the erosion peak may occur at 60° and the erosion rate-impact angle dependence can even be in shape of "N". These were well explained through mechanism analysis. Although TZP had high Kic value (10-20 Kg·mm'), its erosion rates were 6-8 times larger than that of ZTA(Kic: 4.9-6.0 kg·mm'). An empirical equation was derived as follows: $E=a\cdot K^{**}C/HV^{**}.$

Here,m and n varied from 0.5 to 1.4 and 0.13 to 0.35 respectively with different erodents.

(51-SIVP-89C)

STRENGTHS OF MELT-DERIVED HOLLOW ZIRCONIA SPHERES: A. Chung, P. Austin, Univ. Wash., Seattle, WA and R.C. Bradt, Univ. Nev., Peno,

The fracture stress of melt-derived hollow monoclinic zirconia spheres were measured in diametral compression in the as-received state and after annealing at temperatures from 900°C to 1300°C. The strengths and their changes were analyzed using a two-parameter Weibull distribution and the results interpreted in terms of the microstructure and the effects of annealing in the monoclinic to tetragonal transition region.

(50-SIVP-89C)

LASER-INDUCED INTERNAL CRACKING IN Zro, (Yro,) SINGLE CRYSTALS, Z.Y. Wang, M.P. Harmer and Y.T. Chou, Department of Materials Science and Engineering, Lehigh University, Bethlehem, PA 18015

Internal cracking was produced in ZrO, (Y,O) single crystals under irradiation of a focused short-pulse Nd-YAG laser. Microscopic features of the defects formed near the focus of the laser beam were examined using optical and scanning electron microscopy. The irradiated zone was composed of a disordered core and a well-defined, penny-shaped crack along the fracture plane. The characteristics of the internal cracks and formation mechanisms will be discussed in connection with the fracture properties of ZrO, crystals.

The laser-irradiated crystals were further annealed at elevated temperatures for crack healing. The kinetics of the healing process will also be presented.

(52-SIVP-89C)

POSTINDENTATION SLOW CRACK GROWTH AND ITS EFFECT ON MECHANICAL PROPERTY DETERMINATIONS IN ZIRCONIA CERAMICS, Oh-Hun Kwon and J.A. Trogolo, Norton Co., Goddard Rd., Northboro, MA 01532

The postindentation slow crack growth (PI-SCG) was found in the presence of moisture with zirconias: Y-TZP and ZTAs. The transgranular fracture was predominant on the subcritically cracked fracture surface. It has been found that the PI-SCG behavior substantially affect most mechanical property measurements: fracture toughness (Kic), flexural strength, fatique, R-curve behavior, etc. Significantly different mechanical property values from those of ambient atmosphere tests were measured by minimizing the PI-SCG effect using a dried silicon oil. Related issues and implications were discussed with this newly found phenomena.

(53-SIVP-89C)

FRACTURE TOUGHNESS OF Y-TZP, T.K. Brog* and M.J. Readey, Coors Ceramics Company, Golden, CO 80401,303-277-4891

The fracture toughness of several different stabilized zirconias was measured using different test techniques. Preliminary results suggest that the test technique had little effect on the measured fracture toughness of Mg-PSZ. However, large discrepancies were observed for Y-TZP between the indentation-strength in bending (ISB) test and the single-edge notch beam (SENB) test. Fracture toughness data, test parameters and an explanation/discussion of the results will be presented.



STRESS-RUPTURE PERFORMANCE OF Y-TZP MATERIALS AT 600 AND 700C, Jeffrey J. Swab, U.S. Army Materials Technology Laboratory, Watertown, "A

Yttria tetragonal zirconia polycrystal materials (Y-TZPs) have been examined for a variety of structural applications because of a unique combination of high strength and toughness. However, these applications have been limited due to catastrophic degradation of the material between 200 and 400C in the presence of water and, at elevated temperatures (>800C), a lack of strength and load carrying capabilities which are attributed to increased stability of the tetragonal phase. This paper presents the results of a program to examine the long-term stress-rupture performance of several Y-TZP materials at 600 and 700C.

(54-SIVP-89C)

FRACTURE TOUGHNESS OF Y-TZP'S USING BEND BARS, J.T. Beals, C.M.Murray, G.L. Leatherman, and I. Bar-On*, Worcester Polytechnic Institute, Worcester, MA 01609

difficulty of introducing reproducible straight precracks in Y-TZP's often leads to inconsistent fracture toughness measurements. The majority of the methods currently used to measure fracture toughness in these materials are based on curved cracks. This work reports fracture toughness values of a Y-TZP obtained from 3-point bend bars with naturally sharp, straight through thickness cracks. Results indicate consisistent values of fracture toughness can be obtained by this method. The effect of the precrack load level on the measured fracture toughness values was determined. These results are compared to values obtained by other methods.

(54-SIVP-89C)

ACOUSTIC EMISSION DURING MICRO- AND MACRO-CRACK GROWTH Mg-PSZ. G. Gogotsi, A.V. Drozdov, V.O. Galenko, A.I. Fasenko and M.V. Swain, Institute for Problems of Strength Ukranian Academy of Sciences, Kiev-14, USSR and CSIRO Div. of Materials Science and Technology, Clayton Vic. 3168, Australia.

Acoustic emission (AE) of a Mg-PSZ (TS grade) material have been made during 4 point bending and stable crack extension tests. During flexure AE signals increased significantly upon the onset of in-elastic behaviour and were associated with phase transformation and microcracking on the tensile surface. Observations of crack extension in notched bars revealed relatively little AE during initial loading and onset of non-linear behaviour. However on subsequent loadings the number of counts was in reasonable agreement with the extent of crack growth. These observations are discussed in terms of AE emission from phase transformation and crack growth. They are compared with AE behaviour from other materials.

(57-SIVP-89C)

THE INCLUSION-INITIATED FRACTURE IN A TETRAGONAL ZIRCONIA MATRIX, J.Sung, Norton Company, Northboro, MA, 01532-1545. (508) 393-5970.

The high fracture-toughness high thermal-expansion-coefficient and low Young's-modulus combination of the tetragonal zirconia results in a unique case of inclusion-initiated fracture in ceramics. The present study examines the fracture characteristics of the α -alumina inclusions in a tetragonal zirconia matrix. It is found that exclusive inclusion fracture prior to global occurs at ambient fracture temperatures while the subcritical crack growth is observed at elevated temperatures. A stress analysis in consideration of the thermal-, elastic-mismatch and differential fracture-toughness is conducted. The results are in good agreement with the experimental observation.

(59-SIVP-89C)

MICROHARDNESS ANISOTROPY OF m-ZrO₂ SINGLE CRYSTAL, + Z. Li, * Y. Li, Y. Fang, and M. V. Nevitt, Materials Science Division, Argonne National Laboratory, Argonne, IL 60439

The Knoop microhardness of the single crystal m-ZrO2 was measured on the (100) and (010) planes at the indentation load of 1N. The results show that the microhardness of m-ZrO2 are highly dependent on both indentation planes and indentation orientations. The microhardness is from 9.4 GPa in <101>{010} to 5.8 GPa in <010>{100}. One peculiar fracture behavior was observed by Vicker indentation method. The crack always emanates from only one of the four corners of the Vicker indentation impression. The crack propagation direction is [001] on (100) or $[00\overline{1}]$ on $(\overline{1}00)$. This phenomenon as well as the microhardness anisotropy will be discussed in relation to the elastic and plastic properties of the m-ZrO₂.

(58-SIVP-89C)

ELECTRON MICROSCOPY STUDY OF CRACK PROPAGATION IN ZIRCONIA MATERIALS, D. Michel*, L. Mazerolles and R. Portier, CNRS URA 302, C.E.C.M., 15 rue Georges Urbain, 94407 VITRY (France)

Aligned composites consisting of cubic or tetragonal zirconia and another refractory phase (alumina, magnesia, calcium zirconate) are characterized by X-ray diffraction and electron microscopy. Cracks are initiated on particular crystallographic planes by Vickers or Knoop indentation. Preferred directions for crack propagation are determined by SEM and TEM studies and discussed in relation with structural features. Observations of deflection and blocking of cracks at interfaces demonstrate the significant influence of microstructural parameters on the fracture behavior of these composites.

(60-SIVP-89C)

A MODIFIED INDENTATION TECHNIQUE FOR R-CURVE DETERMINATION OF Y-TZP, R.M. Anderson*, L.M. Braun, W.R. Cannon, Department of Ceramics, Rutgers University, Piscataway, NJ

A modified indentation technique has been developed to measure the R-curve of Y-TZP. The method employed allows the crack growth resistance to be measured for short (microns) crack extensions. The plateau toughness for samples fired to 1600° C (ave. grain size 0.7um) was reached after 10-20 microns of crack extension. The plateau toughness value determined with this technique correlates well with chevron notch fracture toughness values if the ellipticity of the indentation flaw is accounted for.

(61-SIVP-89C)

THERMAL SHOCK FRACTURE BEHAVIOR OF ZIRCONIA BASED CERAMICS, M. Shimada and T. Sato, Tohoku University, Sendai, Japan

Thermal shock fracture behavior of zirconia ceramics such as magnesia partially stabilized zirconia, yttria and ceria-doped tetragonal zirconia polycrystals (Y-TZP and Ce-T2P), Y-TZP/Al₂O₃ composites and yttriadoped cubic stabilized zirconia was evaluated by quenching method using water, methyl alcohol and glycerin as quenching media. Thermal shock fracture of samples was proceeded by the thermal stress due to convective heat transfer accompanied by boiling of solvents. Thermal shock resistance of zirconia based ceramics increased with increasing the fracture strength, but that of Y-TZP and Y-TZP/Al₂O₃ composites was anormalously lower than the predicted value, since the toughening mechanism of zirconia by the stress-induced phase tranformation did not sufficiently function against the thermal stress fracture of Y-TZP based ceramics.

"Creep, Fatigue, and Superplasticity"

(62-SIVP-89C)

BRITTLE-DUCTILE TRANSITION IN Y, 0, STABILIZED Zr0, SINGLE CRYSTALS, G. N. Morscher, S. C. Morane, P. Pirouz, and A. H. Heuer, Department of Materials Science and Engineering, Case Western Reserve University, Cleveland, OH.

The onset of bulk plasticity in single crystals of Y_2O_3 -stabilized ZrO_2 — the brittle-ductile transition — has been studied using high temperature microhardness indentation and notched beam bend tests. The differences between these testing methods and the specific slip systems activated wil be discussed.

(63-SIVP-89C)

FATIGUE BEHAVIOR OF CETZP, Y. Kubota*, Tosoh Co., 2743-1, Hayakawa, Ayase-shi, Kanagawa, 252 Japan: M. Ashizuka, Kyushu Institute of Technology, 1-1 sensui-cho, Tobata-ku, Kitakyushu-shi 804, Japan.

Fatigue behavior of tetragonal Zirconia polycrystals containing 12 mol% Ceria were measured by the dynamic fatigue technique at 20° and 250°C. This paper will report the fatigue behavior and discuss in comparison with that of Y-TZP.

(64-SIVP-89C)

FATIGUE OF 3Y-TZP, S.Y. Liu* and I-Wei Chen, Department of Materials Science and Engineering, University of Michigan, Ann Arbor, MI 48109-2136. (313) 763-6661.

Both tension-compression fatigue in uniaxial loading and fatigue crack growth in bending and in compact tension have been studied. These results afford an opportunity to compare the short crack (c.a. 10 to 100 μ m) data and the long crack (c.a. 1cm) data for this class of moderate toughness ceramics. Very strong dependence of fatigue life on stresses are found in all the data. Methodology for life prediction will be illustrated.

(66-SIVP-89C)

INFLUENCE OF ENVIRONMENT ON THE STATIC AND CYCLIC FATIGUE OF Mg-PSZ, M.V. Swain and V. Zelizko CSIRO Division of Materials Science and Technology, Clayton Victoria 3168 Australia

The influence on the static and cyclic fatigue strength of Mg-PSZ Materials has been undertaken in a range of environments. The environments included, stream, HCl, NaOH, Ringer's solution as well as distilled water and air. From the data generated it was found that the strength degradation was much more severe under cyclic loading (R = -1). The results are interpreted in terms of K-V on da/dN-AK relationships on the basis of assuming a specific initial flaw size and by ignoring R-Curve behaviour. However recent observations of small flaw behaviour very different from macrocrack data. Independent observations of crackgrowth rate are compared with the calculated rates from the strength data.

(65-SIVP-89C)

Microstructural Aspects of Monotonic and cyclic Fatigue Cracks in Mg-PSZ, R.H.J. Hannink, M.V. Swain and V. Zelizko, CSIRO, Division of Materials Science and Technology, Locked Bag 33, Clayton, Victoria 3168, Australia.

Recent studies by a number of authors have established that the threshold stress intensity factor for macro crack extension under cyclic loading is much lower than static loading. The aim of this study has been to compare the extent of microstructural damage developed during monotonic and cyclic fatigue crack growth in an endeavour to establish the mechanism responsible for the enhanced fatigue crack growth rate. Comparison of microstructural studies of monotonic and cyclic crack propogation were carried out using optical and electron optical techniques.

(67-SIVP-89C)

CAVITATION STUDY ON SUPERPLASTIC TETRAGONAL ZIRCONIA MATERIAL

P. DESCAMPS, BCRC; F. WAKAI, GIRI 7000 MONS-Belgium NAGOYA 462-JAPAN Superplastic ceramics exhibit extremely large elongations to failure in the tensile deformation. However, nowadays, current interest is mainly focussed on the understanding of the superplastic mechanisms. Very few publication refer to the specific study of the cavitation problem whereas excessive cavitation may lead either to undesirable post-forming characteristics or to premature failure. In this paper, we propose to study the cavitation problem on monostructural zirconia(100% tetragonal phase). Influence of the strain, strain rate and temperature of the tests on the nucleation, growth, interlinkage of cavities and on the cavity morphology will be carefully examined. Application of the theories dealing with those phenomena developed on superplastic alloys will be discussed. Importance of the surface state in the area of the gage length as well as of the alignment of the sample will also be emphasized.

(68-SIVP-89C)

PROCESSING OF FINE YTTRIA-STABILIZED ZIRCONIA POWDERS FOR THE STUDY OF SUPERPLASTICITY M. Ciftcioglu', U'NM/NSF Center For Micro-Engineered Ceramics, University of New Mexico, Albuquerque, NM M.J. Mayo and I.A. Voigt, Sandia National Luboratories, Albuquerque, NM.

It is essential that fine-grained dense ceramics can be prepared for the study of the phenomenon of ceramic superplasticity. Recent studies on the superplasticity of yttria-stabilized zirconia ceramics prepared from a commercial powder have shown that they can be elongated more than 120% with the right combination of strain rate and temperature. The finest commercial powders available have a distribution or particle sizes in the 0.1-1.0 µm range with most of the particles in the $0.2\text{-}0.4~\mu m$ range. In this study finer yttria-stabilized zirconia powders were prepared through coprecipitation. These powders have been characterized and different consolidation techniques were used for the preparation of high density uniform green structures. The densification behaviour of these compacts along with compacts prepared from commercial powders have been studied in the 900-1400 C range. The densified structures were further mechanically tested for the determination of the superplastic behaviour of the pellets. The results of the densification studies along with the mechanical testing data will be presented.

California Pavilion C Anaheim Hilton Friday Morning • November 3

"Mechanical Properties/Microstructural Correlation"

Session Chair: Manfred Rühle, Max-Planck-Institut für Metallforschung, Stuttgart, FRG

8:00-8:40 a.m.-(38-SIV-89C)

PROCESSING AND PROPERTIES OF COMPLEX ZIRCONIA COMPOSITES, N. Claussen* and E. Lutz, Technical University of Hamburg-Harburg, Advanced Ceramics Group, P.O. Box 90 14 03, D-2100 Hamburg 90, Federal Republic of Germany

Y-TZP exhibits the highest room-temperature strength of all polycrystalline ceramics. Its thermoshock resistance, however, especially its retained strength after severe thermal shocks $(\triangle T>\triangle T)$ is relatively low. Dispersion of high m content pressure zones in the TZP matrix enhances K_{TC} , at the expense of strength though, and promotes considerable R increases with crack extension which again improves the retained strength. In some composites microcrack cascading takes place leading to process zone sizes of several millimeters. The cascading phenomenon also occurs adjacent to Vickers indents.

Fracture behavior is discussed with respect to stress analysis data and R-curve behavior is correlated to thermal shock resistance. The potential of this microstructural architecture concept for other ceramic systems is outlined.

8:40-9:00 a.m.—(39-SIV-89C)

Relationship Between Fracture Toughness and Phase Assemblage in Mg-PSZ, R.H.J. Hannink and M.V. Swain, CSIRO, Division of Materials Science and Technology, Locked Bag 33, Clayton, Victoria 3168, Australia; C.H. Howard and E.H. Kisi, A NSTO, Private Bag 1, Menai, NSW 2234, Australia.

9

I

1

Ì

3

I

Magnesia partially stabilised zirconia (Mg-PSZ) is one of the toughest engineering ceramics available. The mechanical properties of Mg-PSZ are achieved through judicious heat treatment below the sub-eutectoid temperature to promote the micro-structural features necessary to achieve the enhanced properties. Development of the delta phase (Mg_Zr_50_1_2) is thought responsible for the superior toughness. The current work seeks to examine the correlation between fracture toughness and volume fractions of the tetragonal and delta phases. The volume fractions of both phases were determined using neutron powder diffraction techniques.

9:00-9:20 a.m.-(40-SIV-89C)

TRANSFORMATION BEHAVIOR IN Ce-T2P COMPOSITES. P. F. Becher, Oak Ridge National Laboratory, Oak Ridge, TN and G. A. Rossi*, Norton Company, Advanced Ceramics Div., Northboro, MA

The transformation temperatures, amount transformed, and the room temperature toughening for alumina containing 30 vol.% zirconia (14 mol% ceria) particles of differing size distributions are described. Reduction of the zirconia size, achieved by decreasing the sintering time at 1600°C, decreased M. temperatures and increased the amount transformed below 22°C. As a result, the transformation toughening contribution at 22°C increases, e.g., $dK_{11}^{I} > 5.5 \text{ MPa.} \sqrt{m} \text{ ob-}$ tained in composites with flexural strengths of 700 MPa.

9:40-10:20 a.m.-(42-SIV-89C)

CRACK TIP ZONES IN TRANSFORMATION TOUGHENED CERAMICS. D.B. Marshall, Rockwell Science Center, Thousand Oaks, CA

Direct measurements of transformation zone characteristics in ZrO2 materials will be discussed and related to theoretical calculations of toughening. Techniques used include Raman spectroscopy for phase content and optical methods for both in-plane and out-of-plane strains within the zone. Results will be used to assess toughening by ferroelastic transformations as well as by the $t \star m$ transformation.

9:20-9:40 a.m.-(41-SIV-89C)

A Novel Toughening Mechanism from Dispersions of Monoclinic Zirconia Polycrystals(MZP),R.C.Garvie,M.F.Goss, S.Marshall,G.T.Mayer and C.Urbani, CSIRO, Division of Materials Science and Technology, Clayton, Victoria, Australia.

Refractories are badly degraded ceramics because of their porosity. The latter is required to induce thermal shock resistance. Traditionally, there has been a trade-off between resistance to thermal shock and corrosion/erosion resistance. Dispersions of MZP in brittle matrices perform the same function as pores; viz, generate localised dense networks of microcracks in regions subject to thermal shock stresses. However, these advanced refractory ceramics are dense and strong as well as thermal shock resistant. The toughening mechanism is unrelated to the phase transformations. A sketch of a proposed theory will be discussed.

10:20-11:00 a.m.-(43-SIV-89C)

R-CURVES OF PSZ AND TZP MATERIAL; ROLE OF MICROSTRUCTURE AND INFLUENCE ON PROPERTIES, M.V. Swain CSIRO Div. of Materials Science and Technology, Clayton Vic. 3168 Australia.

There is now considerable theoretical and experimental data on R-Curve behaviour for transformation toughened ceramics (TTC). Examples of the role of microstructure and heat treatment on the R-Curves for Mg-PSZ, Y-TZP and Ce-TZP are given. Under some circumstances the extent of the R-Curve is very much larger than the transformed zone size about the crack tip. The effect of such R-Curves on the mechanical properties of TTC materials is also discussed.

11:00-11:20 a.m.-(44-SIV-89C)

INFLUENCE OF FAR-FIELD TRANSFORMATION ON R-CURVE BEHAVIOR OF MG-PSZ, R.W. Steinbrech, G. Dransmann, Institut für Reaktorwerkstoffe, KFA Jülich GmbH, FFG, A.H. Heuer, Pepartment of Materials and Engineering, Case Western Reserve University Cleveland, DH, USA

The material response on deflection of bend bars was studied with two grades of MgD partially stabilized zirconia. Both the maximum strength and the maximum toughness zirconia exhibited load relaxation behavior when kept at constant displacement after deformation. However, the effect was more pronounced in the high toughness material. From in situ microscopic observation of the tensile surface the relaxation could be related with far field transformation of tretragonal (t) precipitates to monoclinic (m) symmetry, growth of surface cracks and crack assisted t-m transformation. The cracks experienced an increasing toughness with extension (R-curve effect). The influence of the far field transformation on R-curve behavior is examined.

11:40 a.m.-12:00 noon-(46-SIV-89C)

MECHANICAL PROPERTIES AND LOW TEMPERATURE STABILITY OF POLYCRYSTALLINE t'-ZIRCONIA

J. F. Jue*, K. Mehta, and A. V. Virkar, Dept. MS&E, 304 EMRO, University of Utah, Salt Lake City, UT. 84112.

Presintered (1450°C/4 hrs.) zirconia ceramics with 2 to 8 m.% Y2O3 were annealed at 2100°C. Samples with 3 to 6 m.% Y₂O₃ were tetragonal (t') with grain size between 90 and 200 µm. Electron microscopy revealed the presence of a submicron domain-like structure within the grains. Toughness, strength and hardness were measured. The toughness and the strength of the t'-phase was more than twice that of the cubic phase. No monoclinic phase was detected on as- fired, ground or fracture surfaces. The samples were also aged at 275°C for more than 1000 hrs. These materials (t') did not undergo degradation unlike the t-phase. The results are discussed in terms of ferroelasticity and transformation.

11:20-11:40 a.m.-(45-SIV-89C)

IOW TEMPERATURE DEGRADATION OF Y-TZP MATERIALS, E. Lilley* and A.J. Brandes, Norton Company, Advanced Ceramics, Goddard Road, Northboro, MA 01532

The influence of composition, grain size, surface finish, and HIP'ing on low temperature degradation has been studied in Y-TZP's prepared from arc melted zirconia/yttria. Extensive measurements of the modulus of rupture have been made after exposing the bend bars at 250°C in slightly humid nitrogen, 120°C in water, both for varying times, and at 200°C/100 psi for 50 hours. Where the degraded zone thickness is less than or equal to the preexisting critical flaw size in a bar; little deterioration in strength is experienced.

This work was funded by DOE through ORNL.

"Creep, Fatigue, and Superplasticity"

Session Chair: Anil V. Virkar, Department of Materials Science and Engineering, University of Utah, Salt Lake City, UT

1:00-1:40 p.m.-(47-SIV-89C)

STRENGTHENING AND PLASTIC REFORMATION IN Y-CSZ AND Y-PSZ SINGLE CRYSTALS, A.H. Heuer, K. McClellan, J.M. Martinez-Fernandez, M. Jimdnez-Dedendo and A. Dominguez-Rodriguez, (Invited), Case Western Reserve University, Cleveland OH

Strengthening and plastic deformation in Yttria stabilized ZrO₂ single crystals have been studied above 1200°C. Solid solution strengthening operated in the fully stabilized cubic single crystals, containing 9.4 to 32 mol% Y₂O₃. In the two phase regime, containing 4.5 mol% Y₂O₃, precipitation strengthening is more effective. Serrated flow has been observed in all of the above crystals.

1:40-2:20 p.m.-(48-SIV-89C)

SUPERPLASTICITY OF FINE GRAIN ZIRCONIA POLYCRYSTALS, I-Wei Chen, Department of Materials Science and Engineering, University of Michigan, Ann Arbor, MI 48109-2136. (313)763-6661.

Since the seminal work of Wakai, et al. on superplasticity of 3Y-TZP in 1986, rapid progress has been made in exploring and understanding this phenomenon in zirconia ceramics. A review on the current status of the field will be given here. The effect of crystal structure, additives, grain boundary mobility, and phase distribution will be assessed.

2:20-3:00 p.m.--(49-SIV-89C)

CYCLIC FATIGUE-CRACK PROPAGATION BEHAVIOR IN ZIRCONIA CERAMICS: LONG vs. SMALL CRACK BEHAVIOR.

R. H. Dauskardt, A. A. Steffen, and R. O. Ritchie, Center for Advanced Materials, Lawrence Berkeley Laboratory, and Department of Materials Science and Mineral Engineering, University of California, Berkeley, CA 94720.

Recent studies in engineering ceramics have provided persuasive evidence of degradation and premature failure under cyclic loading. In the present study, cyclic fatigue-crack propagation behavior is investigated in MgO-PSZ, heat treated by sub-sutectoid aging to a range of toughnesses $K_{\mbox{\scriptsize IC}}$ from 2.9 MPa/m (overaged) to 16.0 MPa/m (M5 grade). Where behavior is examined in compact tension specimens containing pre-existing through-thickness long (>2mm) cracks, crackgrowth rates are found to be power-law dependent on the stressintensity range, AK, and to show evidence of a threshold stressintensity range, AKTH, approximately equal to 50% Kin. Conversely, for naturally-occurring small (-1 to 100 µm) surface cracks in unnotched cantilever bend specimens, crack-growth behavior is observed at ΔK levels some 2 to 3 times smaller than the long-crack threshold, similar to behavior observed in metals. Mechanisms of cyclic fatigue in transformation-toughened ceramics are examined and implications for the structural design are discussed.

3:00-3:20 p.m.-(50-SIV-89C)

FATIGUE CRACK PROPAGATION IN CERIA-PARTIALLY-STABILIZED ZIRCONIA (CeO₂-TZP) CERAMIC, J. F. Tsai, C. S. Yu and D. K. Shetty, University of Utah, Salt Lake City, UT

Fatigue crack propagation rates in tension-tension load cycling were measured for a ZrO2-12m% CeO2 ceramic using precracked and annealed compact tension specimens. Crack growth rates in the range 10-10 to 10-5 m/cycle were measured for cyclic stress intensity (ΔK_I) ranging from 8 to 13 MPa. vm. The stress-intensity exponent in a power-law correlation was about 13 at high crack-growth rates. The threshold stress intensity and the range of stress intensity for fatigue crack propagation were comparable to the stress-intensity range for R-curve behavior in monotonic loading. However, the crackgrowth rates and total crack extension were much greater for cyclic loading. Specimen surface observations using Nomarski interference contrast revealed that both the transformation zone width and the zone length ahead of the crack tip were significantly smaller for a cyclically loaded specimen relative to a monotonically loaded specimen when compared at the same maximum applied stress intensity (K_{max}). Reduction of crack shielding by the reduced zone size due to reverse transformation appears to be a mechanism of fatigue crack propagation.

3:20-3:40 p.m.-(51-SIV-89C)

INFLUENCE OF $Y_{2}O_{3}$ CONTENTS AND GRAIN SIZES ON THE FATIGUE BEHAVIOR OF Y-T2P, M. Ashizuka*, Kyushu Insitute of Technology, 1-1, Sensui-cho, Tobata-ku, Kitakyushushi, 304, Japan; Y. Kubota, Tosoh Co., 2743-1, Hayakawa, Ayase-shi, Kanagawa 252, Japan.

Fatigue behavior of tetragonal zirconia polycrystals containing 2, 3 and 4 mol% Y_2O_3 were measured by the dynamic fatigue technique at 20° and 250°C. Crack growth parameters N at 20°C became more than 40 and were not affected by the grain size. The N values of the grain size group of 1 μ m at 250°C became less than 10 while the N values of the group of 0.5 μ m showed a maximum at 3 mol% Y_2O_3 and decreased with decreasing Y_2O_3 contents to 2 mol%. The monoclinic zirconia contents on the fracture surface after fatigue measurement decreased monotonously with increasing Y_2O_3 contents for a certain grain size.

4:09-4:20 p.m.—(53-SIV-89C)

THE ROLE OF GRAIN BOUNDARY GLASS PHASE ON THE SUPERPLASTIC DEFORMATION OF TETRAGONAL ZIRCONIA POLYCRYSTALS, Yu-ichi Yoshizawa and Taketo Sakuma, Department of Material's Science, Faculty of Engineering, The University of Tokyo, 7-3-1 Hongo, Tokyo 113, Japan.

Superplastic deformation of tetragonal zirconia polycrystals (TZP) was investigated by compression test in a temperature range 1100-1400°C. Special attention was paid to examine the role of grain boundary glass phase on the high temperature deformation behavior. The addition of glass phase markedly improved the high temperature deformability. Lithium silicate glass was much superior to alumino-silicate glass and lithiumaluminum silicate glass for decreasing the high-temperature flow stress and for lowering the superplastically-deformed temperature. The decrease of room-temperature strength due to the glass addition was less than 30%. The deformation mechanism of TZP containing grain boundary glass phase will be discussed.

3:40-4:00 p.m.-(52-SIV-89C)

EFFECTS OF ADDITIVES AND IMPURITIES ON SUPERPLASTICITY OF Y-TZP, F. Wakai* and Y. Kodama. Government Industrial Research Institute, Nagoya, Nagoya 462, Japan; T. Nagano, Suzuki Motor Co., Hamamatsu 432-91 Japan; P.G.E. Descamps, 7000 Mons, Belgium; H.Okamura, Nippon Soda Co., Odawara 250-02, Japan.

The grain boundary sliding (GBS) is the major deformation mechanism for the superplasticity of Y_2O_3 -stabilized tetragonal ZrO_2 polycrystals (Y-TZP). The structure of grain boundaries greatly affects the GBS. The tension tests and the tensile creep tests were conducted to investigate the deformation of TZPs with different grain boundary structures (Clean grain boundary, Grain boundary containing thin amorphous film, Grain boundary with intentional addition of impurities).

Ceramic Science and Technology Congress Author Index

In this index, the numbers and letters in parentheses indicate the order of the author's paper within a symposium or similar program; e.g., 2-SXV-89C indicates that it is the second paper to be presented in Symposium XV at the 1989 Congress. The letter "P" following the program indicates that it is a poster presentation.

Paper Coding

SI = Applications for Ceramics in Modern Society SII = Computer Applications in Ceramic Technology SIII = Environmental Issues in Ceramic Technology

SIV = 4th International Conference on the Science and Technology of Zirconia

Symposium on Cement Manufacturing and Chemistry

SVI = Symposium on Ceramic Composites

SVII = Symposium on Commercial Glass Manufacturing and Applications

SVIII = Symposium on Electro-optics and Nonlinear **Optics**

SIX = Symposium on Materials & Processes for Microelectronic Systems

SX = Symposium on Microwave Processing of Ceramics

Symposium on Sol/Gel and Colloidal Processing

Symposium on Superconductivity and Ceramic Superconductors

SXIII = Synthesis of High-Temperature Materials

SXIV = Current Trends in California Dinnerware and Tile

SXV = International Symposium on Corrosion and Corrosive Degradation of Ceramics

F = Fulrath Award Symposium

CL = Ceramic Lecture Series

A
Abe, H., (4-SIII-89C)
Abou-el-leil, M., (64-SIX-89C)
Adams, L., (2-SV-89C), (9-SV-89C),
(10-SV-89C)
Adiga, R., (24-SXV-89C)
Adiga, R., (24-SXV-89C)
Adiga, R., (24-SX-89C)
Adiga, R., (24-SX-89C)
Alon, R., (34-SX-89C)
Ahna, B., (10-SXII-89C)
Ahn, B., (10-SXII-89C)
Ahn, B., (10-SXII-89C)
Ahn, R., (37-SIVP-89C)
Akinger, F., (3-SVIII-89C)
Akazawa, N., (2-SXVP-89C)
Akiba, T., (30-SIVP-89C)
Akiba, T., (30-SIVP-89C)
Akiba, T., (30-SIVP-89C)
Akimoto, S., (13-SIV-89C)
(50-SXI-89C), (53-SXI-89C)
Akimoto, S., (13-SIV-89C)
Alford, N., (64-SXII-89C)
Alford, N., (64-SXII-89C)
Alo, R., (16-SI-89C)
Ameen, M., (18-SVIII-89C)
Amino, T., (12-SXIII-89C)
Amino, T., (12-SXIII-89C)
Anderson, M., (32-SIV-89C)
Anderson, M., (32-SIV-89C)
Anderson, R., (43-SIVP-89C)
Anderson, C., (35-SVI-89C)
Arashi, H., (13-SIVP-89C)
Arashi, H., (13-SIVP-89C)
Arashi, H., (13-SIVP-89C)
Argent, R., (18-SVII-89C)
Argent, R., (18-SVII-89C)
Arullah, S., (21-SIVP-89C)
Arullah, S., (21-SIVP-89C)
Arun, R., (13-SXV-89C)

Arya, P., (20-SXIII-89C), (21-SXIII-89C) Aselage, T., (30-SXII-89C) Ashby, M., (36-SVI-89C) Ashizuka, M., (51-SIV-89C), (63-SIVP-89C) (63-SIVP-89C)
Ashkin, D., (41-SXI-89C)
Asmussen, Jr., J., (6-SX-89C)
Aspholm, G., (5-SVII-89C)
Atwood, J., (15-SXII-89C)
Auborn, J., (3-SVI-89C)
Auciello, O., (18-SVIII-89C)
Axelson, S., (30-SXIII-89C)
Axxoni, C., (35-SIV-89C)

B
Badwal, S., (5-SIV-89C),
 (6-SIVP-89C)
Bailey, A., (15-SIX-89C)
Bailey, P., (31-SIX-89C)
Baker, C., (7-SI-89C)
Baker, D., (7-SI-89C)
Baker, W., (10-SI-89C)
Balachandran, U., (13-SXII-89C),
 (27-SXII-89C), (53-SXII-89C)
Balbaa, I., (10-SX-89C)
Balbaa, I., (10-SX-89C)
Baldoni, G., (57-SVI-89C)
Bandoni, T., (14-SXIII-89C)
Bannister, M., (36-SVI-89C)
Bansal, N., (41-SXII-89C)
Bansal, N., (41-SXII-89C)
Bano, Y., (12-SVIP-89C)
Bao, Y., (12-SVIP-89C)
Baromin, X., (74-SIX-89C)
Bar-Don, I., (45-SVI-89C)
Barbarossa, G., (10-SVIII-89C)
Barger, G., II-SV-89C
Barkatt, Aa., (24-SXV-89C)
Barsoum, M., (34-SVI-89C)
Bateman, A., (33-SIVP-89C)

The American Ceramic Society assumes no responsibility for statements and opinions advanced by the contributors to its publications, or by the speakers at its programs.

Bateman, C., (21-SIV-89C)
Batlogg, B., (2-SXI1-89C)
Baulogg, B., (2-SXI1-89C)
Baukal, C., (3-SVII-89C)
Bayat, G., (4-SII-89C)
Beals, J., (45-SIV-89C)
Beals, J., (45-SIV-89C)
Becals, J., (45-SIV-89C)
Becher, P., (40-SIV-89C)
Beccher, P., (40-SIV-89C)
Beck, J., (13-SXI-89C)
Beck, J., (13-SXI-89C)
Beck, F., (9-SXII-89C)
Beck, F., (9-SXII-89C)
Berlin, G., (11-SVII-89C)
Berlin, G., (11-SVII-89C)
Berlin, G., (11-SVII-89C)
Berry, D., (67-SIX-89C)
Besharatian, P., (3-SII-89C)
Besharatian, P., (3-SII-89C)
Bhalla, A., (56-SXII-89C)
Bhalla, A., (56-SXII-89C)
Bhargava, A., (33-SXII-89C)
Bhargava, A., (33-SXII-89C)
Binnie, D., (16-SVIII-89C),
(39-SIX-89C), (39-SXII-89C)
Bianchard, C., (32-SXI-89C)
Blake, R., (3-SX-89C)
Blanchard, C., (32-SXI-89C)
Blanchard, C., (32-SXI-89C)
Blanchard, C., (32-SXI-89C)
Blanchard, C., (35-SXI-89C)
Bonnell, J., (7-SXII-89C)
Bonnell, J., (7-SXII-89C)
Bornemisza, T., (3-SIX-89C)
Bornemisza, T., (3-SIX-89C)
Bornemisza, T., (3-SIX-89C)
Bowen, H., (36-SIX-89C)
Bowman, K., (45-SIX-89C)
Bowman, K., (14-SIV-89C)
Bowen, H., (36-SIX-89C)
Braun, L., (20-SIX-89C)
Brandes, A., (45-SIX-89C)
Brandes, A., (45-SIX-89C)
Brinker, C., (6-SXI-89C)
Brinker, C., (6-SXI-89C)
Brook, R., (49-SIX-89C)
Burdick, V., (25-SXV-89C)
Burdick, V., (25-SXV-89C) Burton, B., (9-SXII-89C) Burton, L., (52-SIX-89C) Busch, J., (8-SI-89C) Butler, E., (1-SIVP-89C)

Cabera, J., 12-SV-89C Caesar, E., (21-SIVP-89C) Cahn, D., (7-SV-89C) Cai, H., (27-SVI-89C) Camagni, P., (4-SIVP-89C) Camara, M., (3-SVP-89C) Camilo, G., (5-SVIP-89C) Campbell, G., (24-SVI-89C) Canner, J., (17-SIX-89C), (55-SIX-89C) (3)-SIX-89C) Cannon, R., (39-SVI-89C) Cannon, W., (20-SIV-89C), (16-SIVP-89C), (43-SIVP-89C), (60-SIVP-89C) (80-51YP-89C) Cao, H., (40-SVI-89C) Carim, A., (45-SXII-89C) Carlson, R., (40-SIX-89C) Carlson, W., (67-SXII-89C) Carolan, M., (4-SIV-89C) Carpenter, Jr., J., (1)-SX-89C)
Carpenter, Jr., J., (1)-SX-89C)
Carrick, R., (8-SIII-89C)
Carter, D., (34-SIV-89C)
Carty, W., (50-SXI-89C)
Caruso, J., (20-SI-89C) Caruso, J., (20-S1-89C)
Casagramda, A., (9-SVI-89C)
Cava, R., (2-SXII-89C)
Cazzato, A., (66-SXII-89C)
Chaklader, A., (24-SXII-89C)
Chan, C., (19-SIV-89C),
(34-SIVP-89C)
Chan, K., (9-SIVP-89C),
(10-SIVP-89C)

Chan, S., (9-SIV-89C)
Chandler, G., (4-SX-89C)
Chang, J., (39-S1-89C),
(115-SVII-89C)
Chatterjee, A., (33-SVI-89C)
Chen, C., (15-SVII-89C)
Chen, C., (15-SVII-89C)
Chen, H., (40-SXII-89C)
Chen, H., (40-SXII-89C)
Chen, W., (12-SIV-89C)
Chen, W., (12-SIV-89C)
Chen, W., (12-SIV-89C)
Chen, Y., (16-SIVP-89C)
Chen, Y., (16-SIVP-89C)
Cheng, H., (59-SXII-89C)
Cheng, J., (12-SIV-89C)
Cherukuri, S., (21-SIX-89C)
Cherukuri, S., (21-SIX-89C)
Chevalier, J., (44-SXII-89C)
Chiang, C., (7-SXII-89C)
Chiang, Y.-M., (62-SXII-89C)
Chino, M., (57-SIX-89C)
Chino, M., (57-SIX-89C)
Chiu, C., (3-SIX-89C)
Chou, H., (34-SVI-89C)
Chou, H., (34-SVI-89C)
Chou, H., (34-SVI-89C)
Chou, K., (24-SXII-89C)
Chou, K., (25-SXII-89C)
Chu, C., (2-SVIII-89C),
(13-SIX-89C), (12-SXII-89C)
Chu, C., (2-SVIII-89C),
(17-SXIII-89C)
Church, R., (5-SX-89C)
Ciacchi, F., (6-SIVP-89C)
Ciftcioglu, M., (68-SIVP-89C)
Ciftcioglu, M., (68-SIVP-89C)
Ciark, D., (4-SX-89C),
(35-SXIII-89C)
Clark, D., (4-SX-89C),
(35-SXIII-89C)
Clark, D., (4-SX-89C),
(38-SIVP-89C)
Clark, D., (14-SVI-89C)
Clark, D., (15-SXII-89C)
Condrate, Sr., R., (42-SXII-89C)
Cook, R., (14-SVI-89C)
Cook, R., (14-SVI-89C)
Cook, R., (14-SVI-89C)
Cook, R., (16-SXII-89C)
Cors, L., (23-SXII-89C)
Cousino, R., (36-SXII-89C)
Cousino, R., (36-SXII-89C)
Cousino, R., (36-SXII-89C)
Cook, R., (16-SXII-89C)
Cook, R., (16-SXII-89C)
Cook, R., (16-SXII-89C)
Cousino, R., (36-SXII-89C)
Cou (11-SVIII-89C), (12-SIX-89C), (11-SXIII-89C) Croucher, D., (30-SXIII-89C) Culler, J., (50-SXIII-89C) Cutler, R., (11-SIX-89C), (3-SXIII-89C) Czekaj, C., (36-SX1-89C)

D'Ovidio, F., (24-SIV-89C)
Dalgleish, B., (37-SVI-89C),
(39-SVI-89C)
Dalton, A., (3-SVII-89C)
Dalton, R., (35-SXIII-89C)
Damodaran, A., (58-SXII-89C)
Damofit, J., (23-SIVP-89C)
Danforth, S., (27-SXIII-89C)
Dannels, C., (28-SXIII-89C)
Dannels, C., (28-SXIII-89C)
Danyluk, S., (9-SXV-89C)
Das, A., (1-SVP-89C), (2-SVP-89C)
Das Gupta, S., (6-SI-89C),
(37-SI-89C), (27-SIVP-89C)
Dastur, M., (1-SVP-89C),
(2-SVP-89C)
Dauskardt, R., (49-SIV-89C), Dauskardt, R., (49-SIV-89C), (39-SV1-89C) (39.5VI-89C)
Davis, D., (5.5V-89C)
Davis, J., (23.5VI-89C)
Davis, P., (42-SXI-89C)
Davis, P., (42-SXI-89C)
Oavison, W., (22-SXII-89C)
DeGuire, M., (16-SXV-89C)
Debsikdar, J., (17-5XII-89C), (19-5XII-89C)
Decker, L., (4-SXI-89C)
Decker, R., (14-SX-89C)
Degreve, J., (39-SXIII-89C), (15-SXIII-89C)

Demaggio, G., (14-SX-89C) Deobald, L., (15-SVIP-89C) Derep, L., (26-SIV-89C) Descamps, P., (52-SIV-89C), (67-SIVP-89C) Dessemond, L., (7-SIVP-89C) Desu, S., (3-SIX-89C), (7-SIX-89C), (8-SIX-89C), (27-SIX-89C), (37-SIX-89C), (51-SIX-89C), (44-SXI-89C) (8-SIX-89C), (27-SIX-89C), (37-SIX-89C), (37-SIX-89C), (31-SIX-89C), (44-SXI-89C) Dewan, H., (13-SX-89C) Dewan, H., (13-SX-89C) Dewan, H., (13-SX-89C) Dewan, P., (13-SVIII-89C) Diffetto, S., (10-SVI-89C) Diffetto, S., (10-SVI-89C) Diffetto, S., (10-SVI-89C) Diffetto, S., (11-SIVP-89C) Diffetto, T., (11-SIVP-89C) Diffetto, T., (11-SIVP-89C) Dominguez, R., (13-SIXI-89C) Dominguez, R., (36-SXI-89C) Dominguez, R., (36-SXI-89C) Doroudian, M., (48-SIX-89C) Doroschner, S., (27-SXII-89C) Doroschner, U., (1-SXVP-89C) Doty, P., (36-SI-89C) Doughty, D., (36-SIX-89C) Doughty, D., (36-SIX-89C) Doughty, D., (36-SIX-89C) Doughty, G., (36-SIVP-89C) Doughty, G., (36-SIVP-89C) Doughty, G., (36-SIVP-89C) Dreman, J., (6-SIVP-89C) Dreman, J., (6-SIVP-89C) Dreman, J., (6-SIVP-89C) Droby, G., (42-SXI-89C) Droby, G., (42-SXI-89C) Droby, G., (42-SXI-89C) Droby, G., (42-SXI-89C) Dud, J., (35-SI-89C) Dud, J., (35-SI-89C) Dud, J., (34-SIV-89C) Dudo, J., (34-SIV-89C) Duda, J., (35-51-89C)
Duh, J., (44-SIVP-89C)
Dunmead, S., (33-SXIII-89C)
Dunn, B., (12-SVIII-89C)
Durham, S., (13-SXIII-89C)
Dusek, J., (27-SXII-89C) Dutta, S., (28-SXIII-89C) Dwivedi, A., (36-SIV-89C), (4-SXII-89C), (5-SXII-89C)

Earl. W., (42-SXI-89C)
Ebbers, C., (7-SVIII-89C)
Edirisinghe, M., (57-SXI-89C)
Eggestedt, P., (11-SI-89C)
Egolf, J., (40-SXI-89C)
Eichelberger, C., (40-SIX-89C)
Eimerl. D., (7-SVIII-89C)
Einloth, M., (53-SXII-89C)
Eleazer, P., (35-SVII-89C)
Ellingson, W., (8-SII-89C)
Ellingson, W., (8-SII-89C)
Ellis, D., (37-SIV-89C)
Emerson, J., (13-SXII-89C) Ellis, D., (37-SIV-89C)
Ellis, D., (37-SIV-89C)
Emerson, J., (13-SXII-89C)
Emery, A., (13-SXII-89C)
Endo, Y., (10-SXIII-89C)
Endo, Y., (10-SXIII-89C)
Engell, J., (23-SIVP-89C)
Epperson, J., (9-SIV-89C)
Epperson, J., (9-SIV-89C)
Eror, N., (13-SXII-89C)
Evans, A., (9-SVI-89C), (21-SVI-89C), (23-SVI-89C), (21-SVI-89C), (23-SVI-89C), (38-SVI-89C)
Evans, E., (8-SVI-89C)
Evans, G., (24-SVI-89C)
Evans, G., (24-SVI-89C)
Evans, G., (24-SVI-89C)
Evans, G., (53-SXI-89C)
Exarhos, G., (53-SXI-89C)
Ezis, A., (47-SVI-89C)

Faber, K., (27-SVI-89C)
Falk, L., (25-SIV-89C)
Falk, L., (25-SIV-89C)
Fang, Y., (9-SIV-89C),
(59-SIVP-89C)
Fastnozzi, G., (9-SVIP-89C)
Fassina, P., (28-SXI-89C)
Fazzan, P., (13-SXI-89C)
Federer, J., (27-SXV-89C)
Feng, G., (16-SIVP-89C)
Feng, X., (24-SXV-89C)
Fergus, J., (3-SXV-89C)
Fergus, J., (3-SXV-89C)
Feuston, B., (51-SXI-89C)
Fincher, C., (31-SXII-89C)
Fincher, C., (9-SXIII-89C)
Fitch, L., (25-SXV-89C)
Fitcher, M., (1-SXI-89C)
Fiter, E., (2-SXV-89C)
Fletcher, M., (1-SXI-89C)
Flinn, B., (8-SVI-89C)

Flinn, D., (38-SV1-89C) Flores, D., (20-SI-89C) Folsom, C., (11-SV1-89C) Ford, R., (63-SNII-89C) Founder, M., (26-SIV-89C) Founder, M., (26-SIV-89C) Fox, B., (25-SIX-89C) Fox, D., (14-SXV-89C) Fox, J., (19-SXI-89C) Frattrez, P., (27-SXIII-89C) Frederick, L., (24-SXIII-89C) Fredericksen, J., (23-SIVP-89C) Fredericksen, J., (23-SIVP-89C) Freman, S., (20-SIX-89C) Fremen, R., (37-SIV-89C) French, R., (37-SIV-89C) French, R., (37-SIV-89C) French, R., (37-SIV-89C) French, R., (37-SIV-89C) Fryburg, G., (5-SI-89C) Flinn, D., (38-SVI-89C) Fryburg, G., (5-SI-89C) Fuchs, H., (34-SIV-89C) Fuchs, H., (34-SIV-89C) Fueng, F., (29-SIVP-89C) Fujii, K., (2-SIVP-89C) Funii, T., (44-SVI-89C), (4-SIX-89C) Fukunaga, O., (28-SIX-89C) Fukunaga, O., (28-SIX-89C) Fuller, E., (7-SXII-89C) Fuqua, P., (12-SVIII-89C) Fuyi, L., (34-SI-89C)

Gar, P., (61-SXII-89C) Gai, P., (61-SXII-89C)
Gaines, M., (5-SIII-89C)
Galenko, V., (56-SIVP-89C)
Gang, P., (31-SXIII-89C)
Gangolli, S., (5-SXI-89C)
Garcia, D., (24-SIVP-89C)
Garcia, R., (36-SXI-89C)
Gardner, J., (34-SIV-89C)
Garnio, I., (22-SVI-89C), (56-SIX-89C)
Garotalini, S., (51-SXI-89C)
Garvie, R., (41-SIV-89C), (10-SIVP-89C)
Gavulic, J., (14-SX-89C) Gavulic, J., (14-SX-89C) Gerhardt, R., (20-SIV-89C) Gerling, J., (7-SX-89C) Ghodgaonkar, D., (13-SX-89C) Ghosh, D., (6-SI-89C), (37-SI-89C), (27-SIVP-89C) Gnodgaoirat, D., (13-5X-89C)
Ghosh, D., (6-SI-89C), (37-SI-89C),
(27-SIVP.89C)
Giess, E., (3I-SIX-89C)
Gintewicz, J., (27-SVIII-89C)
Ginterner, C., (47-SVIII-89C)
Giszpenc, N., (47-SVII-89C)
Giszpenc, N., (47-SVII-89C)
Glasser, A., (61-SXI-89C)
Glasser, A., (61-SXI-89C)
Glass, A., (28-SVIII-89C)
Goog, C., (53-SVII-89C)
Goog, C., (53-SVII-89C)
Googy, C., (35-SIVP-89C)
Googlan, K., (8-SII-89C)
Googlan, K., (28-SXII-89C)
Googlan, C., (18-SVIII-89C)
Googlan, C., (18-SVIII-89C)
Googlan, C., (18-SVIII-89C)
Googlan, C., (18-SVIII-89C)
Grader, G., (40-SXII-89C)
Grader, G., (40-SXII-89C)
Grader, G., (40-SXII-89C)
Grader, G., (41-SVIII-89C)
Green, D., (41-SVIII-89C)
Green, D., (41-SVIII-89C)
Groscom, D., (11-SVIII-89C)
Groscom, D., (11-SVIII-89C)
Groves, K., (36-SI-89C)
Groves, K., (36-SI-89C)
Guyta, P., (8-SXV-89C)
Gupta, T., (35-SIX-89C)
Gupta, T., (35-SIX-89C)
Gupta, T., (35-SIX-89C)
Gupta, T., (35-SIX-89C)
Gur, T., (10-SXII-89C)
Gusman, M., (46-SXII-89C) Gur, T., (10-SXII-89C) Gusman, M., (46-SXII-89C)

Haber, R., (3-SVI-89C), (41-SXI-89C) Hadet, N. 1.39 (1-38), (41-5X1-89C)
Hackett, J., (41-5X1-89C)
Hartling, G., (41-5X11-89C)
Hahn, H., (11-5XYP-89C)
Hallock, R., (15-5X11-89C)
Hallock, R., (15-5X11-89C)
Halverson, D., (34-5X11-89C)
Halverson, D., (34-5X11-89C)
Hannink, R., (39-51V-89C), (65-51VP-89C)
Hannink, R., (39-51V-89C)
Harrada, H., (54-51X-89C)
Harkins, B., (14-51X-89C)
Harris, J., (7-511-89C)
Hartshorn, A., (21-51VP-89C)
Hartzell, C., (18-5X1-89C) Hashimoto. N., (14-SXIII-89C)
Hassler, Y., (12-SX-89C)
Haught, D., (50-SXII-89C)
Hav, R., (45-SXI-89C)
Hayashi, M., (44-SXI-89C)
Hayashi, I., (18-SXII-89C)
Hayashi, I., (18-SXII-89C)
Hezlebeck, D., (49-SXI-89C)
Hetter, J., (7-SII-89C)
Heitzman, R., 13-SV-89C
Henager, Jr., C., (11-SXV-89C)
Hendricks, R., (60-SVI-89C)
Hermandez, D., (4-SVIP-89C)
Hermandez, D., (4-SVIP-89C)
Hermandez, D., (44-SVIP-89C)
Heuer, A., (18-SIV-89C),
(33-SIV-89C), (44-SIV-89C),
(47-SIV-89C), (62-SIVP-89C)
Heussner, K., (38-SIVP-89C)
Heystek, H., (10-SVIP-89C)
Hill, M., (54-SXII-89C)
Hill, R., (10-SIV-89C)
Hill, R., (10-SIV-89C)
Hill, R., (10-SIV-89C)
Hill, R., (10-SIV-89C)
Hill, R., (10-SXIII-89C)
Hishinuma, K., (30-SIVP-89C)
Hishinuma, K., (30-SIVP-89C)
Hodgson, D., (46-SXII-89C)
Hodgson, D., (46-SXII-89C)
Hodgson, D., (46-SXII-89C)
Hollosi, L., (15-SI-89C)
Holl, J., (1-SXIII-89C)
Hollosi, L., (15-SI-89C)
Holt, J., (1-SXIII-89C)
Homeny, J., (50-SVI-89C) (33-SXIII-89C) Homeny, J., (50-SVI-89C) Honda, F., (28-SXII-89C) Hong, D., (3-SXII-89C) Hong, L.-H., (21-SXI-89C) Hong, W., (24-SIX-89C) Hoppe, M., (17-SXI-89C) Horowitz, H., (31-SXII-89C), (2-CL-89C) Hoppe, M. (1 - S.M. - 89C)
Horowitz, H., (3) - S.MI - 89C),
(2-CL - 89C)
Houchin, M., (2 - SIII - 89C),
(25-SIVP - 89C)
Howard, C., (10-SIV - 89C),
(39-SIV - 89C)
Hseuh, C., (32-SVI - 89C),
(43-SVI - 89C), (6-SVIP - 89C)
Hu, Y., (34-SXII - 89C)
Huang, C.-L., (21-SXI - 89C)
Huang, C.-L., (21-SXI - 89C)
Huang, S., (39-SI - 89C),
(36-SIVP - 89C)
Huang, Y., (17-SIVP - 89C)
Huang, Y., (17-SIVP - 89C)
Hudson, A., (8-SII - 89C)
Huebner, W., (4-SIX - 89C)
Huggins, R., (10-SXII - 89C)
Hurley, Jr., W., (36-SXI - 89C)
Hurley, Jr., W., (36-SXI - 89C)
Hwang, C., (45-SIX - 89C)
Hwang, S.-S., (23-SVIII - 89C)

Ibaraki, Y.. (10-5XIII-89C) Ichikawa, H., (34-5IX-89C) Ichikawa, H., (34-5IX-89C) Ichinose, A., (60-5XII-89C) Ichinose, N., (21-5XII-89C) Idorn, G., (1-5X-89C) Idorn, G., (1-5X-89C) Ikawa, H., (28-5IX-89C) Ikawa, H., (28-5XII-89C) Ikeda, J., (62-5XII-89C) Ikeda, S., (5-XIII-89C) Imai, H., (35-SIX-89C) Imoto, F., (22-5XI-89C) Interrante, L., (36-5XI-89C) Interrante, L., (36-5XI-89C) Inix, K., (12-5XIII-89C) Inix, K., (12-5XIII-89C) Inixiawa, A., (20-5IVP-89C) Ishitam, A., (20-5IVP-89C) Ishitam, A., (20-5IVP-89C) Ishitam, A., (37-5XI-89C) Isoda, T., (37-5XI-89C) Isoda, T., (37-5XI-89C) Iwahara, H., (16-5XI-89C) Iwahara, H., (16-5XI-89C) Izawa, H., (5-5XIII-89C)

Jacobs, J., (37-S1-89C), (27-SIVP-89C) (27-SIVP-89C)
Jacobson, N., (14-SXV-89C)
Jada, S., (24-SIV-89C)
Jada, S., (24-SIV-89C)
Jain, M., (48-SVI-89C)
Jenkins, D., (25-SIVP-89C)
Jensen, R., (46-SIX-89C),
(47-SIX-89C)
Jeong, B., (33-SIX-89C)
Jeong, J., (22-SIV-89C)
Jessen, T., (25-SVI-89C)
Jiang, C., (32-SI-89C)
Jiang, Q., (67-SIX-89C)
Jimdnez-Dedemdo, M.,
(47-SIV-89C) (47-SIV-89C) Jin, S., (40-SXII-89C)

Jin. Z., (2-SVIP-89C), (12-SVIP-89C)
Johansen, V., (1-SV-89C)
Johnson, D., (11-SIX-89C), (11-SX-89C), (36-SXII-89C)
Johnson, Jr., D., (40-SXII-89C)
Johnson, S., (13-SXII-89C), (46-SXII-89C)
Jones, R., (11-SXV-89C), (17-SXV-89C)
Joshi, A., (2-SIV-89C)
Jue, J., (46-SIV-89C)
Juhlin, N., (19-SVI-89C)
Justus, B., (14-SVIII-89C)

Kaga, T., (28-SIVP-89C)
Kahn, M., (42-SIX-89C)
Kajinami, A. (15-SXIII-89C)
Kajiwara, T., (54-SIX-89C)
Kajiszewski, M., (18-SIV-89C)
Kamas, J., (5-SV-89C)
Kameda, T., (51-SVI-89C)
Kanaji, Y., (15-SXIII-89C)
Kanbara, E., (15-SXIII-89C)
Kanbara, E., (15-SXIII-89C)
Kanda, A., (34-SIX-89C)
Kaneko, S., (22-SXI-89C)
Kaneko, S., (29-SIVP-89C)
Karasek, K., (46-SVI-89C)
Karasek, K., (46-SVI-89C)
Karasek, K., (46-SVI-89C)
Karasek, K., (46-SVI-89C)
Kato, N., (34-SIX-89C)
Kato, S., (60-SIX-89C)
Kato, S., (60-SIX-89C)
Kato, T., (28-SIVP-89C)
Kato, T., (3-SX-89C)
Kawamura, N., (37-SXI-89C)
Kawamura, N., (37-SXI-89C)
Kawamura, S., (10-SXIII-89C)
Kawamura, S., (12-SIVP-89C)
Kaya, H., (17-SXII-89C) Nawamura, T., (10-SXIII-89C)
Kawasaki, S., (12-SIVP-89C)
Kava, H., (37-SXI-89C)
Kazemzadeh, A., (48-SIX-89C)
Keareney, J., (13-SVII-89C)
Kearns, R., (29-SVI-89C)
Kearens, R., (29-SVI-89C)
Keat, W., (17-SXIII-89C)
Keeskes, L., (37-SXIII-89C)
Keeskes, L., (37-SXIII-89C)
Keeter, K., (30-SXII-89C)
Keut, R., (1-SXIV-89C)
Kent, R., (17-SXII-89C)
Kennish, R., (17-SXII-89C)
Kennish, R., (17-SXI-89C)
Kim, D., (22-SIV-89C)
Kim, H., (45-SIX-89C)
Kim, H., (45-SIX-89C)
Kim, H., (45-SIX-89C)
Kim, W.-S., (33-SIX-89C)
Kim, W.-S., (33-SIX-89C)
King, G., (30-SIX-89C)
Kingman, D., (33-SXIII-89C)
Kingman, D., (33-SXIII-89C)
Kingman, D., (33-SXIII-89C)
Kister, J., (57-SXII-89C)
Kistano, Y., (20-SIVP-89C)
Kistano, Y., (20-SIVP-89C)
Kistano, Y., (20-SIVP-89C)
Kiettz, M., (7-SVII-89C)
Klettz, M., (7-SVII-89C)
Klettz, M., (7-SVII-89C)
Klettz, M., (7-SVII-89C)
Klette, M., (7-SVII-89C)
Klette, M., (7-SVII-89C)
Kobayashi, R., (7-SXII-89C)
Kodama, T., (27-SXII-89C)
Kodama, T., (27-SXII-89C)
Kodama, T., (27-SXII-89C)
Kodama, T., (25-SXIII-89C)
Kodama, T., (25-SXIII-89C)
Kodek, W., (9-SX-89C)
Kolbeck, W., (9-SX-89C)
Komatsu, M., (51-SVII-89C)
Komatsu, M., (51-SVII-89C)
Komatsu, M., (51-SVII-89C)
Kopang, R., (4-SVII-89C) Kawasaki, S., (12-SIVP-89C) Kaya, H., (37-SXI-89C) (1-F-89C)
Konsztowicz, K., (41-SIVP-89C)
Koppang, R., (4-SVII-89C)
Koshimura, M., (20-SXII-89C)
Kosugi, N., (25-SXIII-89C)
Kottke, T., (37-SXIII-89C)
Kramlich, J., (4-SVII-89C)
Krasevec, V., (9-SIX-89C)
Kratzer, R., (14-SXI-89C)
Kratzer, R., (14-SXI-89C)
Kratzer, E., (51-SXII-89C)
Kreider, E., (51-SXII-89C)
Kreider, E., (51-SXII-89C)
Kreider, E., (51-SXII-89C)
Krupanidhi, S., (20-SVIII-89C)

Kubo, H., (44-SVI-89C), (*0-SIX-89C) Kubota, Y., (51-SIV-89C), (63-SIVP-89C), (25-SXIII-89C) Kudoh, Y., (13-SIVP-89C) Kugimiyo, K., (2-F-89C) Kuhliger, C., (24-SXIII-89C) Kumak, T., (30-SIVP-89C) Kumar, K., (58-SXII-89C) Kume, S., (12-SIVP-89C) Kumar, K., (58-SXII-89C) Kume, S., (12-SIVP-89C) Kumta, P., (31-SI-89C), (20-SXI-89C) Kurosky, R., (12-SXI-89C) Kuwaima, J., (1-SVIP-89C) Kuwaishima, H., (20-SIVP-89C) Kwok, C., (44-SXI-89C)

LaGraff, J., (42-SXII-89C) Laine, R., (17-SXI-89C) Lalevic, B., (47-SXII-89C) Lam, D., (37-SIV-89C) Lambropoulos, J., (13-SIV-89C), (23-SVIII-89C) Lambropoulos, J., (13-SIV-89C), (23-SVIII-89C)
Lamoreaux, R., (46-SXII-89C)
Lanagan, M., (13-SXII-89C), (33-SXII-89C), (33-SXII-89C), (10-SVI-89C), (19-SIV-89C), (19-SIV-89C), (19-SIV-89C), (19-SIV-89C), (21-SVI-89C), (21-SVI-89C), (21-SVI-89C), (25-SXI-89C), (25-SXI-89C), (31-SXI-89C), (55-SXI-89C), (54-SXI-89C), (55-SXI-89C), (54-SXI-89C), (54-SXI-89C), (54-SXI-89C), (54-SXI-89C), (54-SXI-89C), (54-SXI-89C), (54-SXI-89C), (54-SXI-89C), (55-SXI-89C), (54-SXI-89C), (55-SXI-89C), (55-SXI-(13-SVIP-89C)
Lee. C.-H., (43-SIX-89C)
Lee. S., (18-SXV-89C)
Lee. V., (10-SXII-89C)
Lessing, P., (3-SIX-89C)
Leu, H., (66-SXII-89C)
cung, D., (19-SIV-89C),
(34-SIVP-89C) (34-51VF-89C) Levinson, L., (40-51X-89C) Lewis, D., (25-5VI-89C) Li, C., (3-51X-89C), (37-51X-89C) Li, T., (11-51VP-89C). (18-51VP-89C), (19-51VP-89C) Li, V., (43-SVI-89C) Li, X., (12-SVIP-89C) Li, Y., (16-SIVP-89C) Li, Z., (9-SIV-89C), (9-SIVP-89C), Li, Z., (9-SIV-89C), (9-SIVP-89C), (9-SIVP-89C), (99-SIVP-89C) Limatta, W., (16-SXIII-89C) Liles, K., (10-SVIP-89C), (23-SXV-89C), (23-SXV-89C) Limave, S., (12-SI-89C) Lin, C., (24-SXI-89C) Lin, L., (11-SXI-89C) Lin, L., (11-SXI-89C), (15-SVI-89C), (10-SXI-89C), (10-S Lin, W., (32-SI-89C), (15-SVI-89C), (10-SXI-89C) Lindemanis, A., (1-SII-89C) Ling, H., (16-SIX-89C) Ling, S., (32-SIV-89C) Ling, S., (32-SIV-89C) Liu, L., (46-SXII-89C) Liu, Q., (28-SIV-89C) Liu, Q., (28-SIV-89C) Liu, W., (54-SIVP-89C) Liu, W., (57-SVI-89C) Loehman, R., (42-SVI-89C), (29-SXIII-89C) Loehman, K., (42-SV1-89C), (29-SXII-89C)
Logan, K., (2-SXIII-89C)
Longo, C., (37-SIV-89C)
Longo, E., (24-SIVP-89C)
Lougher, W., (62-SIX-89C)
Louty, R., (7-SV1-89C), (38-SV1-89C), (59-SV1-89C), (21-SXIII-89C), (21-SXIII-89C), (21-SXIII-89C)
Lumet, J., (26-SIV-89C)
Lundgren, C., (52-SV1-89C)
Luthra, K., (10-SXV-89C)
Luttra, K., (10-SXV-89C)
Luttra, C., (33-SIV-89C)
Lyman, C., (33-SIV-89C)
Lyman, C., (33-SIV-89C)
Lynch, A., (13-SXI-89C)
Lynsdale, C., 12-SV-89C

MacDowell, J., (23-SIX-89C) Macedo, P., (24-SXV-89C) Maciver, D., (9-SV-89C)

Mackenzie, J., (21-SVIII-89C).
(33-SXII-89C), (13-SXII-89C).
(68-SXII-89C), (16-SXIII-89C)
Macda, T., (55-SXII-89C)
Mah, T., (33-SVI-89C),
(23-SXIII-89C)
Mahonev, M., (7-SII-89C)
Majorowski, S., (6-SXIII-89C)
Manson, S., (16-SXIII-89C),
(55-SIX-89C)
Marshaul, P., (36-SXI-89C)
Martinez, S., (30-SXIII-89C)
Marshail, D., (32-SIV-89C)
Martinez, S., (56-SIX-89C)
Marshail, T., (20-SIV-89C)
Masaki, T., (20-SIV-89C) Martinez, S., (56-SIX-89C)
Martinez-Fernandez, J.,
(47-SIV-89C)
Masaki, T., (20-SIVP-89C)
Masaki, T., (20-SIVP-89C)
Masson, T., (6-SXII-89C)
Masson, C., (30-SIV-89C)
Massuda, S., (14-SXI-89C)
Matsuda, S., (14-SXI-89C)
Matson, L., (23-SXIII-89C)
Matson, L., (23-SXIII-89C)
Matson, L., (23-SXIII-89C)
Matsuo, Y., (14-SVIP-89C)
Mayon, M., (16-SIVP-89C)
Mayor, M., (16-SIVP-89C)
Mayor, M., (16-SIVP-89C)
Mayor, W., (16-SIVP-89C)
Mazorolles, L., (58-SIVP-89C)
Mazerolles, L., (58-SIVP-89C)
Mazerolles, L., (58-SIVP-89C)
McCandlish, L., (47-SYII-89C)
McCallan, K., (48-SIV-89C)
McGinn, P., (32-SXII-89C)
McLauphin, K., (4-SXI-89C)
McMerano, R., (5-SXII-89C)
McMerano, R., (5-SXII-89C)
Mehta, K., (46-SIX-89C)
Mehta, K., (46-SIX-89C)
Mehta, K., (4-SIX-89C)
Merzhanov, A., (57-SXII-89C)
Messong, G., (4-SIX-89C)
Mieve, D., (17-SXII-89C)
Mikeska, K., (46-SIX-89C)
Milev, D., (17-SXII-89C) (44-5X11-89C) Mikeska, K., (46-SIX-89C), (47-SIX-89C) Miley, D., (17-SXII-89C), (19-SXII-89C) Miley, D., (17-5XII-89C), (19-5XII-89C) Miller, E., (4-5V-89C) Miller, E., (4-5V-89C) Miller, M., (24-5VIII-89C), (25-5VIII-89C), (25-5VIII-89C), (4-5XIII-89C), (4-5XIII-8 (25-SXIII-89C)
Mort. Y., (20-SIVP-89C)
Mortr. P., (6-SVIII-89C)
Mortscher, G., (62-SIVP-89C)
Mort. G., (36-SI-89C)
Moulson, A., (49-SVI-89C)
Mova, J., (9-SVIP-89C)
Moztarzadeh, F., (33-SI-89C),
(38-SI-89C), (4-SII-89C),
(2-SIVP-89C), (3-SIVP-89C),
(48-SIX-89C), (25-SXI-89C),
(26-SXI-89C)

Mullen, R., (60-SVI-89C) Munir, Z., (32-SXIII-89C), (33-SXIII-89C), (34-SXIII-89C) Munson, M., (5-SIX-89C) Muran, Y., (27-SVIII-89C) Murano, K., (26-SVIII-89C) Murdock, S., (3-SXIV-89C) Muto, N., (54-SIX-89C)

Nagano, T., (\$2-\$IV-89C)
Nagle, D., (8-\$IVP-89C)
Nahass, P., (36-\$IX-89C)
Nakai, Z., (30-\$IVP-89C)
Nakayama, Y., (34-\$IX-89C)
Nakayasu, T., (26-\$XIII-89C)
Nanataki, T., (22-\$XI-89C)
Narita, H., (28-\$IX-89C)
Narita, H., (28-\$IX-89C)
Nebe, W., (41-\$IX-89C)
Neff, G., (16-\$VII-89C)
Neff, G., (16-\$VII-89C)
Netson, R., (42-\$IX-89C)
Nemat-Nasser, S., (15-\$IV-89C)
Nettleship, I., (19-\$IV-89C)
Netugaonkar, R., (27-\$I-89C),
Neurgaonkar, R., (27-\$I-89C) Nettleship, I., (19-SIV-89C), (34-SIVP-89C)
(34-SIVP-89C)
Neurgaonkar, R., (27-SI-89C), (5-SVIII-89C), (24-SVIII-89C), (25-SVIII-89C), (25-SVIII-89C), (25-SVIII-89C), (59-SIVP-89C)
Nevitt, M., (9-SIVP-89C), (32-SIX-89C)
Nicoli, D., (30-SXI-89C)
Nicoli, D., (30-SXI-89C)
Nicoli, D., (30-SXI-89C)
Nighan, W., (64-SIX-89C)
Nighan, W., (64-SIX-89C)
Nighan, W., (64-SIX-89C)
Nighan, W., (64-SIX-89C)
Nikhah, B., (3-SIII-89C)
Nikhida, F., (12-SVIII-89C)
Nishida, F., (12-SVIII-89C)
Nishida, F., (12-SVIII-89C)
Nishikawa, T., (3-SVIP-89C)
Nishikawa, T., (3-SVIP-89C)
Niwa, T., (14-SVIP-89C)
Noda, H., (37-SXI-89C)
Noda, H., (37-SXI-89C)
Noda, T., (7-SIV-89C)
Norman, C., (1-SIVP-89C)
Norman, C., (1-SIVP-89C)
Notis, M., (21-SIV-89C)
Notis, M., (33-SIVP-89C)
Notis, M., (33-SIVP-89C)
Notis, M., (33-SIVP-89C)
Notis, M., (33-SIX-89C)
Nozaki, S., (34-SIX-89C)

O'Bryan, H., (40-SXII-89C)
Obitu, M., (28-SIVP-89C)
Oda, K., (22-SXV-89C)
Oda, S., (10-SX-89C)
Ogata, T., (1-SVIP-89C)
Oh, T., (39-SVI-89C)
Ohmura, K., (27-SVIII-89C)
Ohno, Y., (8-SXII-89C)
Ohuchi, F., (37-SIV-89C)
Ohyanagi, M., (5-SXIII-89C)
Ojo, B., (16-SI-89C)
Okamura, H., (52-SIV-89C),
(55-SIX-89C)
Okazaki, K., (6-SIX-89C), (5)-51X-89C)
(bazaki, K., (6-51X-89C),
(20-5X1I-89C)
Okuyama, M., (8-5XI-89C)
Olaide, G., (4-5VIP-89C)
Oliver, J., (27-51-89C),
(5-5VIII-89C) (5-5VIII-89C)
Omenetto, N., (4-SIVP-89C)
Onada, K., (49-SVI-89C)
Ono, M., (20-SXII-89C)
Onoda, G., (73-SIX-89C)
Oshimoto, A., (57-SIX-89C)
Otsuka, N., (49-SVI-89C)
Ovando, R., (24-SXIII-89C)
Oye, C., (24-SIVP-89C)

Pacey, P., (30-SIV-89C)
Paclorek, K., (14-SXI-89C)
Pagano, N., (20-SVI-89C)
Pai Verneker, V., (8-SIVP-89C)
Painer, R., (15-SXI-89C)
Palanth, D., (2-SXI-89C)
Paleari, A., (35-SIV-89C)
Palmonari, C., (7-SIII-89C)
Paquette, E., (26-SVI-89C)
Paquette, E., (26-SVI-89C)
Parise, J., (61-SXII-89C)
Park, C., (18-SXV-89C)
Park, D., (9-SXV-89C)
Park, J., (33-SIX-89C)
Park, S.-J., (43-SIX-89C)

Partch, R., (5-SXI-89C), Partch, R., (5-SXI-89C), (8-SXIII-89C)
Parthasarathy, F., (23-SXIII-89C)
Pask, J., (42-SVI-89C), (29-SXIII-89C)
Patel, D., (10-SVII-89C)
Payne, D., (7-SIX-89C), (8-SIX-89C), (27-SIX-89C), (151-SIX-89C)
Pearson, D., (59-SXI-89C)
Pegg, J., (24-SIX-89C)
Petetis, N., (24-SIX-89C)
Pemberton, J., (2-SIX-89C)
Pemberton, J., (6-SII-89C) Pentecost, J., (6-SII-89C) Pentecost, J., (6-SII-89C) Peterson, G., (64-SXII-89C) Petuskey, W., (7-SVIP-89C) Phule, P., (13-SVIII-89C), (2-SIX-89C) (2-SIX-89C)
Piconi, C., (28-SXI-89C)
Piconi, C., (28-SXI-89C)
Pilgrim, S., (15-SIX-89C)
Pirouz, P., (62-SIVP-89C)
Plante, E., (19-SXV-89C)
Poeppel, R., (13-SXII-89C),
(26-SXII-89C), (27-SXII-89C),
(26-SXII-89C), (66-SXII-89C)
Porter, J., (55-SVI-89C)
Porter, R., (58-SIVP-89C)
Price, D., (64-SIX-89C)
Price, J., (28-SXV-89C),
(29-SXV-89C)
Puszynski, J., (6-SXIII-89C),
(40-SXIII-89C)
Pytros, N., (59-SXII-89C)

Ruhle, M., (8-SVI-89C) Radonne, L., (39-SXI-89C) Rataniello, W., (11-SXIII-89C) Rahaman, M., (2-SVI-89C) Raj, R., (25-SXII-89C) Rao, C., (1-SXII-89C) Rao, C., (1-SXII-89C)
Rathnamma, D., (15-SXV-89C)
Ratto, J., (55-SVI-89C)
Rawal, B., (18-SIX-89C),
(20-SIN-89C)
Rawn, C., (9-SXII-89C)
Raynes, A., (20-SIX-89C)
Readey, D., (4-SXV-89C)
Reimanis, I., (37-SVI-89C)
Remmele, W., (2-SXV-89C)
Requena, J., (9-SVIP-89C)
Reyes-Morel, P., (15-SIVP-89C),
(42-SIVP-89C)
Rhine, W., (36-SIX-89C), Reves-Morel. P., (15-SIVP-89C), (42-SIVP-89C)
Rhine, W., (36-SIX-89C), (19-SXI-89C), (14-SXII-89C), (15-SXII-89C)
Riman, R., (5-SIX-89C), (27-SXIII-89C)
Risbud, S., (31-SI-89C), (13-SVIII-89C), (2-SIX-89C), (13-SVIII-89C), (2-SIX-89C), (19-SXI-89C), (20-SXI-89C)
Ritchie, R., (49-SIV-89C), (19-SVI-89C)
Robert, J., (4-SIV-89C)
Robinos, W., (36-SIX-89C)
Robinos, W., (36-SIX-89C)
Robinos, W., (36-SIX-89C)
Robinos, L., (4-SIII-89C)
Rogers, W., (15-SIV-89C)
Roddan, J., (31-SIX-89C)
Roman, W., (64-SIX-89C)
Rose, D., (7-SXIV-89C), (10-SXIV-89C)
Rosenthal, A., (59-SXII-89C)
Rosenthal, A., (59-SXII-89C) KOSC. D., (1-5-XIV-89C.), (10-SXIV-89C.)
Rosenthal, A., (59-SXII-89C.)
Ross, J., (6-51-89C.)
Rossi, G., (40-SIV-89C.)
Roth, R., (9-SXII-89C.)
Rothman, S., (26-SXII-89C.)
Routbort, J., (26-SXII-89C.)
Roy, R., (15-SVIII-89C.)
Roy, R., (15-SVIII-89C.), (38-SXII-89C.)
Royere, C., (4-SVIP-89C.), (38-SXII-89C.)
Royston, J., (65-SXII-89C.)
Rubio O., J., (8-SXII-89C.)
Rubio O., J., (8-SVIII-89C.)
Rubic, M., (19-SIV-89C.), (34-SIV-89C.), (41-SVI-89C.), (34-SIV-89C.), (41-SVI-89C.)
Ruller, J., (14-SVIII-89C.)
Ruler, J., (1-SIII-89C.)

Sacks, M., (69-SIX-89C), (56-SXI-89C) (56-SXI-89C) Safari, A., (28-SXII-89C), (29-SXII-89C), (35-SXII-89C), (47-SXII-89C) Saha, C., (22-SXIII-89C) Safa, M., (24-SI-89C), (19-SVIII-89C) Saito, T., (6-SXIV-89C), (10-SXIV-89C)

%kabe, Y., (14-SIX-89C), (17-SIX-89C) (17-SIX-89C)
Sakakibara, N., (4-SIII-89C)
Sakata, K., (37-SXII-89C)
Sakuma, T., (53-SIV-89C)
Sakurai, C., (8-SXI-89C)
Sakuyama, K., (55-SXII-89C)
Salamo, G., (24-SVIII-89C),
(25-SVIII-89C) Salamity, G. 124-SV(1)
Salsman, J., (5-SX-89C)
Salsman, J., (5-SX-89C)
Sambasivan, S., (7-SVIP-89C)
Samogija, G., (4-SIVP-89C)
Samogija, G., (4-SIVP-89C)
Samoels, W., (53-SXI-89C)
Sanchez-Carambot, E.,
(67-SIX-89C)
Santiago-Aviles, J., (67-SIX-89C)
Sartago-Aviles, J., (67-SIX-89C)
Sathre, C., (5-SXI-89C)
Sathre, C., (5-SXI-89C)
Sato, T., (61-SIVP-89C),
(21-SXV-89C)
Savona, J., (10-SIII-89C)
Savona, J., (10-SIII-89C) Savrin, E., (62-S1X-89C), (72-S1X-89C)
Sawada, Y., (14-SXIII-89C)
Sawhil, H., (46-SIX-89C)
Schallotti, M., (4-SIVP-89C)
Schallotti, M., (4-SIVP-89C)
Schilling, C., (53-SXI-89C), (54-SXI-89C), (55-SXI-89C)
Schilling, C., (53-SXI-89C)
Schmidt, H., (2-SXI-89C)
Schoenlein, L., (11-SXV-89C)
Schoenlein, L., (11-SXV-89C)
Schoenlein, L., (11-SXV-89C)
Schoenlein, J., (85-S189C)
Schwab, S., (32-SXI-89C)
Scott, G., (20-SI-89C)
Scott, G., (20-SI-89C)
Scott, R., (19-SI-89C)
Searcy, A., (54-SVI-89C)
Searcy, A., (54-SVI-89C)
Seghi, R., (19-SI-89C)
Sellers, C., (17-SXII-89C), (19-SXII-89C)
Sellers, C., (23-SXI-89C) (19-5X11-89C)
Selmi, F., (23-5X1-89C)
Selvaduray, G., (62-SX1-89C)
Sengupta, S., (2-SII-89C)
Seyferth, D., (34-SXI-89C)
Shahriari, M., (48-SXII-89C)
Shahriari, M., (48-SXII-89C)
Shahriari, M., (48-SXII-89C)
Shanker, K., (13-SXIII-89C)
Shaw, M., (24-SXII-89C)
Shaw, M., (28-SVI-89C)
Shaw, M., (28-SVI-89C)
Shaw, T., (73-SIX-89C)
Shears, B., (8-SXIV-89C)
Shen, Z., (11-SIVP-89C), (10-SXIV-89C)
Shen, Z., (11-SIVP-89C)
Shetty, D., (50-SIV-89C)
Shetty, D., (50-SIV-89C)
Shetty, D., (50-SIV-89C)
Shin, C., (47-SXII-89C)
Shin, C., (47-SXII-89C)
Shin, C., (47-SXII-89C)
Shinda, M., (61-SIVP-89C)
Shinda, M., (61-SIVP-89C)
Shinde, S., (49-SXII-89C)
Shinde, S., (49-SXII-89C)
Simmada, M., (65-SV-89C)
Simpon, M., (18-SVI-89C)
Sigel, Jr., G., (48-SXII-89C)
Sigel, Jr., G., (48-SXII-89C)
Sigengilitt, R., (2-SX-89C)
Simpson, M., (18-SVI-89C)
Singh, J., (53-SXII-89C)
Singhai, S., (1-SIV-89C)
Singhai, S., (14-SXII-89C)
Skibska, M., (38-SXIII-89C)
Skibska, M., (38-SXIII-89C)
Skibska, M., (38-SXIII-89C)
Skibska, M., (38-SXIII-89C)
Sircar, A., (8-SVII-89C)
S

Snyder, H., (2-SVII-89C) Snyder, R., (33-SXII-89C) Solati Hashini, M., (38-SL89C) Solier, J., (33-SIV-89C) Somiya, S., (7-SIV-89C), (5-SIVP-89C), (14-SIVP-89C), (30-SIVP-89C) (5-SIVP-89C), (14-SIVP-89C), (30-SIVP-89C), (30-SIVP-89C), (34-SIV-89C) Sommers, J., (34-SIV-89C) Sorbel, M., (55-SXI-89C) Sparks, J., (48-SXI-89C) Sparrow, J., (2-SXIII-89C) Sparrow, J., (2-SXIII-89C) Spotz, M., (19-SXI-89C) Spotz, M., (19-SXI-89C) Strangle, G., (50-SXI-89C) Stample, G., (50-SXI-89C) Steinbrech, R., (44-SIV-89C) Steinbrech, R., (44-SIV-89C) Streckert, H., (49-SXI-89C) Su, J., (32-SI-89C) Su, H., (34-SIV-89C) Su, M.-Y., (6-SXII-89C) Subramanian, M., (61-SXII-89C) Subramanian, M., (61-SXII-89C) Subramanian, M., (70-SIX-89C) Sukumar, V., (36-SXI-89C) Sukumar, V., (36-SXI-89C) Sung, J., (57-SIVP-89C) Suvorov, D., (9-SIX-89C) Suvorov, D., (9-SIX-89C) Suvar, Y., (30-SIVP-89C) Swain, M., (39-SIV-89C), (66-SIVP-89C), (66-SIVP-89C), (66-SIVP-89C), (66-SIVP-89C) Swartz, S., (17-SVIII-89C)

Tajima, Y., (14-SVIP-89C) Takada, N., (10-SIX-89C) Takada, T., (62-SXII-89C) Takahashi, T., (10-SIX-89C), (3-F-89C) Takenaka, S., (12-SX][1-89C)
Takenaka, T., (37-SX][1-89C)
Talmy, I., (50-SX][1-89C)
Tamaura, Y., (4-SI[1-89C),
(27-SX]-89C) Tanaka, S., (55-SX11-89C), (60-SX11-89C) Tanaka, S., 155-SX11-89C), (60-SXI1-89C)
Tandon, G., (20-SV1-89C)
Tandon, G., (20-SV1-89C)
Tanabata, K., (4-SXIII-89C)
Tarasevich, B., (53-SX1-89C), (55-SX1-89C)
Taylor, J., (23-SX11-89C)
Taylor, J., (23-SX11-89C), (42-SX11-89C)
Telschow, K., (17-SX11-89C)
Telschow, K., (17-SX11-89C)
Tenaglia, A., (7-SIII-89C)
Tenaglia, A., (7-SIII-89C)
Teter, J., (50-SXI1-89C)
Teter, J., (50-SXI1-89C)
Theingaard, N., (58-SX1-89C)
Theory, I., (7-SIX-89C)
Theory, I., (7-SIX-89C)
Thomas, M., (1-SIVP-89C)
Thomas, M., (1-SIVP-89C)
Thorne, K., (16-SXII-89C)
Tien, T., (8-SIV-89C)
Tien, T., (8-SIV-89C)
Tokiwa, K., (27-SVIII-89C)
Tomia, A., (42-SVI-89C)
Tomia, A., (42-SVI-89C)
Tomardi, C., (61-SXII-89C)
Tortecilia, R., (29-SXII-89C) Torardi, C., (61-5X)1-89C)
Torrecillas, R., (9-5V)P-89C)
Tremblay, S., (48-5V)-89C)
Tressler, R., (1-5XV-89C),
(6-5XV-89C)
Trectiles, T., (6-5), (6-5) (15-3AV-89C) Troczynski, T., (6-SI-89C), (37 SI-89C) Trumble, K., (4)-SVI-89C) Tsai, J., (50-SIV-89C) Tsai, M., (17-SXIII-89C) Tsai, T., (11-SVIII-89C) Isan, 1., (11-5VIII-89C)
Tsamopoulos, J., (12-5VI-89C)
Tsuchida, J., (15-5I-89C)
Tsuji, T., (4-5III-89C)
Tucker, D., (48-5XI-89C)
Tunekawa, Y., (16-5XI-89C)
Tuttle, B., (56-5IX-89C)
Tzabari, Y., (8-5VIP-89C)

Uchino, K., (27-SVIII-89C)

Ueki, M., (44-SVI-89C) Ueyama, T., (20-SXII-89C) Uhlman, D., (16-SVIII-89C), (39-SXII-89C) Urbimann, D., (39-SIX-89C) Ulmer, J., (12-SVII-89C) Urabe, K., (5-SXIII-89C) Urashima, K., (14-SVIP-89C) Urbani, C., (41-SIV-89C)

Van Roode, M., (28-SXV-89C), (29-SXV-89C) (29-SXV-89C)
Van de Voorde, M., (12-SXV-89C)
Van der Biest, O., (7-SXV-89C)
Van der Steen, A., (22-SIVP-89C)
Varadan, V. K., (13-SX-89C),
(23-SXI-89C)
Varadan, V. V., (13-SX-89C),
(23-SXI-89C)
Varadan, V. V., (13-SX-89C),
(23-SXI-89C) varadan, V. V., (13-SX-89C), (23-SXI.89C)
Varela, J., (24-SIVP-89C)
Varma, H., (58-SXII.89C)
Varner, J., (52-SXII-89C)
Varshneya, A., (21-SIX-89C)
Vasilos, T., (10-SVI-89C)
Vaughn, G., (3-SIII.89C)
Vaughn, G., (3-SIII.89C)
Vayenas, C., (31-SIV-89C)
Velkov, V., 3-SVP-89C
Velkov, V., 3-SVP-89C
Vilk, P., (1-SVII-89C)
Villafuerte-Castrejon, M., (8-SVIII-89C), (24-SXIII-89C)
Villafuerte-Castrejon, M., (12-SI-89C), (11-SIV-89C), (11-SIV-89C) (3-53/11-89C) Virkar, V., (46-SIV-89C) Voeller, C., (30-SXIII-89C) Voigt, J., (68-SIVP-89C)

Wachtman, J., (41-SXI-89C), (28-SXII-89C) (28-SXII-89C)
Wada, T., (60-SXII-89C)
Wada, Y., (63-SIX-89C)
Wadasworth, J., (55-SVI-89C)
Wakino, K., (14-SIX-89C),
(67-SIVP-89C)
Wakino, K., (14-SIX-89C),
(55-SIX-89C)
Waller, D., (59-SXII-89C)
Waller, D., (59-SXII-89C)
Wang, C., (10-SXI-89C),
(11-SXI-89C)
Wang, J., (39-SIVP-89C),
(25-SXII-89C), (48-SXII-89C)
Ward, R., (67-SXII-89C)
Ward, R., (67-SXII-89C)
Ward, R., (67-SXII-89C)
Wang, S., (50-SVI-89C),
(20-SXV-89C)
Wang, X., (2-SVIP-89C),
(33-SXII-89C), (52-SXII-89C)
Wang, X., (19-SIVP-89C)
Warner, D., (5-SIX-89C)
Warner, D., (5-SIX-89C)
Warner, K., (58-SXII-89C)
Washburn, M., (30-SXIII-89C)
Washburn, M., (30-SXIII-89C)
Watanabe, M., (14-SVIP-89C)
Weber, C., (7-SXV-89C)
Weber, C., (7-SXV-89C)
Weber, C., (6-SI-89C)
Weber, G., (6-SI-89C)
Webern, J., (27-SIV-89C)
Weber, A., (4-SI-89C)
Weber, A., (4-SI-89C)
Weber, A., (4-SI-89C)
Weber, C., (28-SI-89C)
Wetheler, C., (28-SI-89C)
Whetler, R., (1-CL-89C)
Whiteley, B., (23-SXII-89C)
Wilson, C., (29-SXII-89C)
Wilson, C., (29-SXII-89C)
Wilson, C., (29-SXII-89C)
Wilson, C., (29-SXII-89C)
Wister, J., (15-SIX-89C)
Withers, J., (15-SIX-89C)
Withers, J., (7-SVI-89C), (13-SVII-89C), (20-SXIII-89C), (21-SXIII-89C), (21-SXIII Wojnarowski, R., (40-SIX-89C)
Wolfe, H., (7-SVII-89C)
Wong, M., (51-SXII-89C)
Wong, M., (51-SXII-89C)
Wong, G., (24-SVIII-89C)
Wood, G., (24-SVIII-89C),
(25-SVIII-89C)
Woodhead, J., (3-SXI-89C)
Word, W., (14-SVII-89C)
Worrell, W., (6-SIV-89C),
(28-SIV-89C), (3-SXV-89C)
Wu, F., (10-SXI-89C)
Wu, M., (4-SIX-89C)
Wu, M., (4-SIX-89C)
Wu, W., (35-SI-89C), (29-SIV-89C)
Wu, Y., (44-SIVP-89C)

X

Xu, R., (21-SVIII-89C), (43-SXII-89C) Xu, Y., (21-SVIII-89C)

Yagi, T., (13-SIVP-89C) Yamada, O., (4-SXIII-89C) Yamagishi, T., (2-SXVP-89C) Yamaguchi, H., (15-SI-89C) Yamaguchi, T., (35-SIX-89C), (60-SIX-89C), (61-SIX-89C), (63-SIX-89C) (60-S1X-89C), (61-S1X-89C), (63-S1X-89C), (63-S1X-89C) Yamamoto, T., (57-S1X-89C), (20-SX11-89C) Yamaaka, T., (12-S1VP-89C) Yamao, T., (26-SX111-89C) Yamauchi, H., (55-SX11-89C) Yan, M., (16-S1X-89C) Yan, M., (16-S1X-89C) Yang, J., (15-SV1-89C) Yang, J., (15-SV1-89C) Yang, J., (10-SX1-89C) Yang, J., (10-SX1-89C) Yang, J., (10-SX1-89C) Yannone, M., (9-SV-89C) Yanovaka, M., (25-SX11-89C) Yao, P., (32-S1-89C) Yao, P., (32-S1-89C), (11-SX1-89C), (11-SX1-89C) Yashima, M., (7-S1V-89C), (5-S1VP-89C), (14-S1VP-89C) Yazdan-Rad, R., (33-S1-89C), (2-S1VP-89C) (2-SIVP-89C)
Yey, H., (46-SVI-89C)
Yi, H., (36-SXIII-89C)
Yoden, Y., (14-SXIII-89C)
Yogo, T., (16-SXI-89C)
Yonchev, H., 3-SVP-89C
Yongji, P., (31-SXIII-89C)
Yoo, S.-E., (44-SIX-89C)
Yoon, D., (22-SIV-89C)
Yoshikawa, S., (32-SIX-89C)
Yoshimura, M., (7-SIV-89C), (14-SIVP-89C), (30-SIVP-89C), (44-SIX-89C) (44-SIX-89C) (44-SIX-89C)
Yoshio, T., (22-SXV-89C)
Yoshizawa, Y., (53-SIV-89C)
Young, A., (31-SXI-89C)
Young, K., (52-SVI-89C)
Youngdahl, C., (13-SXII-89C)
Youngdahl, K., (17-SXI-89C)
Yu, C., (50-SIV-89C)
Yuli, C., (35-SIVP-89C)

Z

Zachariah, M., (7-SXIII-89C)
Zaghini, N., (28-SXI-89C)
Zelizko, V., (65-SIVP-89C),
(66-SIVP-89C)
Zeng, Z., (17-SIVP-89C)
Zhang, Z., (17-SIVP-89C)
Zhang, Z., (11-SVII-89C)
Zhang, Z., (17-SXI-89C)
Zhang, Z., (17-SXI-89C)
Zhang, Z., (17-SXI-89C)
Zhang, Z., (17-SXI-89C)
Zheng, Q., (17-SIVP-89C)
Zheng, Q., (17-SIVP-89C)
Zheng, Q., (17-SIVP-89C)
Zheng, Z., (1-SXV-89C)
Zhou, A., (2-SVIP-89C)
Zhou, A., (2-SVIP-89C)
Zhow, T., (29-SIV-89C)
Zievers, E., (11-SI-89C)
Zievers, J., (11-SI-89C)
Zievers, J., (11-SI-89C)
Zimmermann, C., (8-SXIII-89C)
Ziyu, L., (34-SI-89C)
Zok, F., (8-SVI-89C)
Zybura, A., (25-SIX-89C)